

COWES HARBOUR COMMISSIONERS

**Sediment Management in the Medina Estuary
Monitoring Results 2019**

Report AmbCHC08

R. S. Nunny BSc. PhD.

FINAL REPORT

April 2020



Contents

Executive Summary.....	2
1. Introduction	4
2. Methods.....	5
2.1 Approach.....	5
2.1.1 Total Suspended Solids Monitoring.....	5
2.1.2 Water Level Monitoring.....	7
2.1.3 Storm Event Monitoring	7
2.1.4 Outer Harbour Water Flow Prediction.....	7
2.1.5 Annual Change in Harbour Bed Levels.....	9
2.2 Effects of Dredging.....	10
2.3 Reconciling Flux and Bathymetry Data	10
3. Results.....	11
3.1 The 2019 Total Suspended Solids (TSS) Regime.	11
3.1.1 Tidal Processes.....	11
3.1.2 Annual TSS Statistics	12
3.1.2 Tidally-Induced Variability in TSS.....	16
3.1.3 Storm-Induced Variability in TSS.....	22
3.1.4 Dredging and Shipping Impacts.	27
3.1.5 Inter-annual Variability	29
3.2 Bathymetric Change.....	31
3.2.1 Quality Control.....	31
3.2.2 2019 Quantitative Summary	32
3.2.3 Local Spatial Variability	34
3.3 Fine-Sediment Flux.....	40
3.3.1 Experimental Options and Assumptions.....	40
3.3.2 Patterns and Processes of Fine-Sediment Flux.....	41
4. Conclusions and Recommendations.....	48
APPENDIX 1. Listing of Excel Files Containing Analysis of Data for 2019 Fine-Sediment Flux Monitoring.	52
APPENDIX 2. Notes on allowing for dredging in sediment budgets.	53



Executive Summary

Measurements of fine sediment dispersion through and around the Medina estuary have been made since January 2016. This report covers the fourth year of monitoring, 1st January-31st December 2019. The monitoring is feeding an understanding of the estuary fine-sediment regime, and is being undertaken to facilitate a more sustainable approach to the management of dredging in the estuary, including the real-time monitoring of the suspended sediment regime during any trials of new dredge methods. The monitoring also addresses the long-term effects upon the fine-sediment regime of the harbour arising from the installation of the new offshore breakwater in 2016.

The monitoring methodology involves continuous field observations of total suspended solids made at four sites within the estuary, annual (December) precision bathymetric surveys of the harbour bed and the combination of these two datasets (together with data on water flow around the harbour) to quantify the flux of mud through the estuary over the year. The scientific objectives are to determine temporal patterns in the processes of fine-sediment accumulation and erosion within the estuary (subdivided into seven polygons) and to add precision to the quantification of spatial patterns of mud accumulation and erosion occurring over the whole year.

The monitoring continues to confirm the conclusions drawn from initial studies undertaken in 2015-16. These indicated that the principle source of mud to the estuary is from winter erosion of the seabed and coast of the wider Wight region of the English Channel, providing a clay-rich material from the Oligocene strata that outcrop in that area. Significant inter-annual variability in this input can be expected and 2019 probably saw a slightly higher than average mud supply, based on regional storm wave records. Continuing slight local erosion of the bed within the estuary (south and east of the new breakwater) provides a secondary input of mud (identifiable from its high silt/low clay content). This erosion is thought to have been exacerbated by the emplacement of the new breakwater, with rates of change steadily decreasing since a 2016 high. However erosion in this zone increased again in 2019, possibly as a result of continuing effects of the breakwater's presence, but most likely due to the dredging of a new Eastern Approach Channel early in the year, with the removal of some 34,000m³ of sediment (predominantly mud). Although dredge volumes are excluded from the sediment flux computations, which attempt to reflect only natural processes, inaccuracies in measuring dredged sediment volumes, together with the processes of stabilisation of disturbed dredged surfaces after the cessation of extraction, probably explain the increased erosion seen in 2019.

Tidal flow, principally over spring tides, is the main agent of fine sediment redistribution within the estuary and is most active during and in the months immediately following the influx of winter mud from offshore (highest during the latter part of the year in 2019). Storms (wind, wave and rain action) play a lesser role, with effects most seen in the vicinity of the harbour entrance. Shipping/boating activity was also seen to enhance turbidity in 2019, causing at times a level of suspended sediment increase approaching that effected by storms.



The outer harbour (between the new breakwater and the chain ferry) lost in total some 1,100 dry tonnes of sediment over the year 2019. Results from the upper estuary (above the chain ferry narrows) indicate accretion of ~3,700 dry tonnes of mud in that zone, the net change for the estuary as a whole being a gain of some 2,500 dry tonnes of fine sediment. Historically the estuary is known to naturally import mud each year (being artificially over-deepened), requiring dredging of the order of 10,000 dry tons per year (averaged over many years). 2019 therefore saw a much decreased input (compared with the more normal input seen in 2018), although accretion still occurred in the known long-term sink zones for mud (marinas, subtidal zone below Shrape Flats). A trend of steady passage from slightly eroding to slightly accreting conditions is also observed at many zones within different parts of the estuary, although the impact of this local shallowing is not reflected in the total changes . The nearshore zone in the eastern approaches to the Medina estuary continues to see increases in sand-bed levels, possibly related to the new breakwater emplacement, with a significantly greater level of sand build-up in 2019 compared to previous years.

Recommendations have been made related to continued improvement the monitoring system/methodology.



Sediment Flux Measurement in the Medina Estuary Monitoring Results 2019

1. Introduction

The monitoring of fine-sediment flux through the Medina Estuary was initiated by Cowes Harbour Commissioners (CHC) in January 2016. This work is a new and experimental approach to monitoring of mud erosion and sedimentation, which is primarily being undertaken with the aim of enhancing the ability for future dredging requirements within the estuary to be managed on a more sustainable basis. The work also addresses a need to monitor the long-term effects of new offshore breakwater. The results of the first year of sediment flux monitoring was published in August 2017¹, with the results from subsequent years (2 and 3) in April of 2018 and 2019 respectively. The monitoring design was based upon previous surveys^{2 3} undertaken in the lower parts of the Medina estuary to provide a detailed conceptual appreciation (model) of the local processes of sediment transport. These reports should be consulted for a full background to the monitoring programme.

Two complementary approaches to quantifying fine sediment movement are used. The first is annual bathymetric change, with surveys conducted in December of each year. The second involves bringing together near-continuous monitoring data of water turbidity at four key sites in the lower estuary with patterns of water-volume exchange around the estuary, to give a time-series of fine-sediment exchanges between seven polygonal zones contained within the lower estuary. Comparing and merging the two sets of results is hoped to provide the best method of quantifying fine-sediment flux into, out of and through the Medina estuary.

Some success was achieved with this experimental approach in the from the initial (2016) dataset. During 2017 and 2018 shortcomings in the practicality of collecting near continuous turbidity data became evident, seriously limiting the accuracy of the flux analyses that could be undertaken. These problems were addressed at the end of 2018 by the installation near-real-time logging systems at the four sensor sites, significantly improving the ability to collect good quality data.

This report covers the fourth year of sediment flux monitoring, from 1st January to 31st December 2019. New data and methods that came available during 2019 are described, addressing both the logging technology and improved analytical procedures that have been followed. The results cover the statistics of the observed suspended sediment regime, changes in the bathymetry of the estuary and the derived fine-sediment flux patterns and tonnages.

¹ Ambios 2017. Sediment Flux Measurements in the Medina Estuary. Monitoring Results 2016. Report AMBCHC03a. August 2017

² Ambios 2016. Sedimentary Processes in the Medina Estuary May 2016 Report AmbCHC02

³ Ambios 2017. Sediment Management in the Medina Estuary: Monitoring Results 2016. Report AmbCHC03. March 2017



2. Methods

2.1 Approach

2.1.1 Total Suspended Solids Monitoring.

Water turbidity data is logged at four sites within the lower Medina Estuary (Figure 1) at five-minute intervals. These optical measures are calibrated to gravimetric (mg l^{-1}) total suspended solids (TSS) values. The data are measured from near mid-depth at each site, following the assumption (based on 2015 turbidity profiling results) that there is no significant vertical stratification in the TSS values.

The raw data from these sensors is transmitted via the internet every 15 minutes⁴. Continuity of high-quality data is threatened principally by biofouling of the optical sensors, and by power failure. Servicing (cleaning) of the sensors is undertaken by CHC staff on a fortnightly basis, or when the internet record shows a problem is occurring. Through the year about 6% of the potential number of turbidity readings were lost (compared with 55% loss in 2018, Table 1). The 2019 loss was primarily due to the failure of the sensor deployed at Shrape, with there then being a fault in the newly purchased replacement sensor (which had to be returned to the manufacturer). A temporary self-logging sensor was deployed to cover this extended downtime period, however this failed to record at one time and then was lost, explaining the significant amount of data loss at Shrape (22%, Table 1). The sensors at the other three sites suffered only about 1% loss:

- Power failure. Three of the sensors have small 12v batteries charged by a mains supply, giving 1-2 days of power in the event of a mains cut. Unfortunately at all three of these sites, for various reasons, the mains power was cut. The buoy sensor at Shrape relies on a solar cell for power, which unfortunately is slightly too small leading to some short power-down periods during cloudy periods in December and January.
- Staff availability. This dictated that on several occasions servicing took place several days after notification of a fault (usually at weekends).
- Weed/biota contamination of the optical windows. The Medina estuary has proven very productive in biofouling terms particularly through the late spring and summer (April – September). During this period copper-film is applied to the sensor bodies and the wiper-arm, which greatly improves the situation. However fouling still occurs and relies upon a prompt response to clean it away once noticed.

Importantly, the short periods of downtime and the high quality of the record at other times made it possible to accurately predict and ‘infill’ the missing data points during 2019, providing a more robust input to the fine sediment flux modelling project.

A system of template Excel workbooks (Appendix) was used to clean and process all the (5 minute) turbidity observations from the four sites over the one-year period, together with water level (tide-hour, tide range) and storm-day data simultaneously recorded water levels. The turbidity data were then grouped into 15-minute values, representing the average and minimum of the three grouped values. The grouped data was then loaded into a standardised Excel workbook, together with the control data (servicing history, local wind and wave data, dredging records). The data were compared with storm and dredging timetables, and occasional spurious average values were either deleted or replaced by the minimum value, if the latter was more realistic. This ‘cleaning’ process is designed to remove the effects of biofouling, in particular the temporary effect of weed strands in

⁴ At the Shrape site this interval was increased to 6 hours, to accommodate solar cell power generation limitations during cloudy winter days.



the water, a problem at certain times of the year in the Medina estuary, often difficult to clearly identify.

	2018			2019
	Loss due to power failure, sensor repair and staff shortages	Loss due to biofouling	Total loss	Loss
SHRAPE	50%	12%	62%	22%
TRINITY LANDING	40%	10%	50%	1.7%
COWES YACHT HAVEN	29%	4%	33%	0.8%
MMC DIVERS	64%	11%	75%	0%

Table 1. Turbidity data loss during 2018 and 2019. Expressed as % of total possible readings that could be taken at each site.

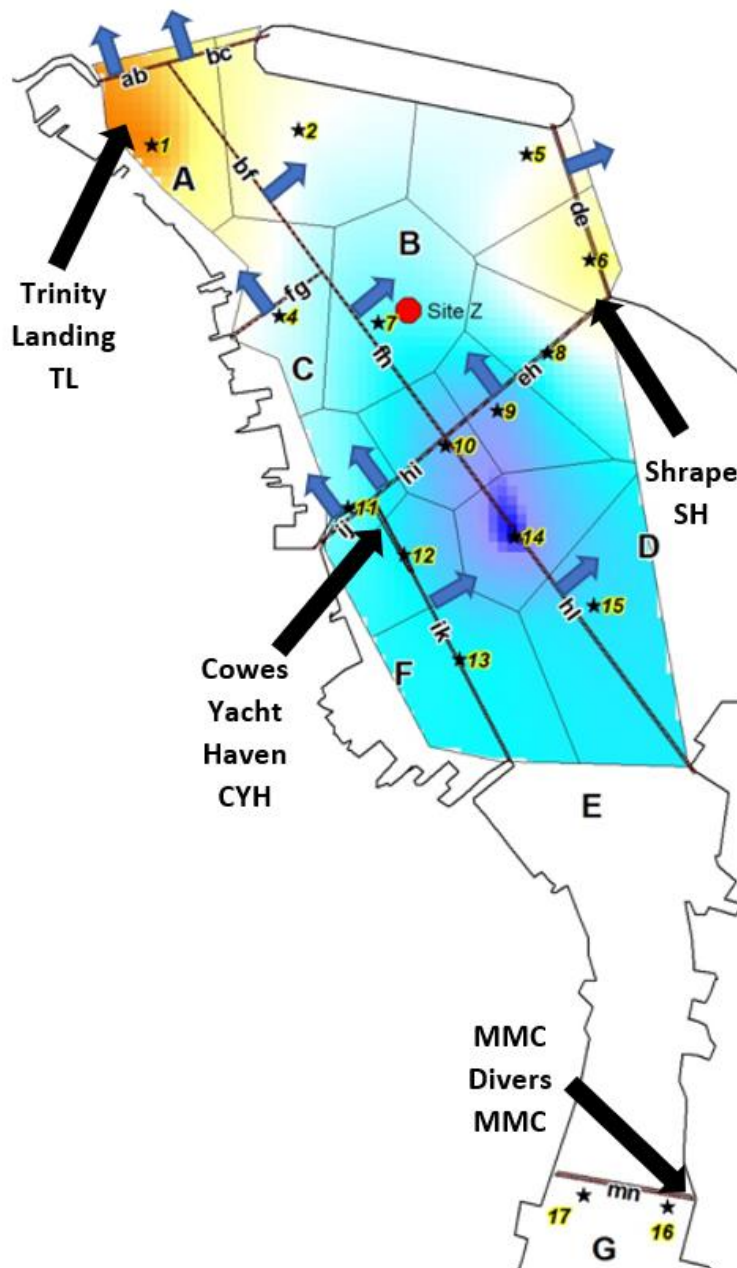


Figure 1. Locations in the lower Medina estuary.

The four turbidity monitoring sites are shown by black arrows. The seven flux polygons (A-G) are shown with thick dark borders, each of the 12 polygon boundaries is labelled in lower case (ab, bc etc).

The 16 Lowell current meter sites are shown as stars, each site is encompassed by a polygon defining its area of principle effect (Voronoi zone).

The coloured grid shows an example of a GIS interpolation of the values of the (E or N) flow components between the measuring sites, derived from analysis of the current meter data. Brown tones show positive flow, blue tones negative flow; the blue arrows show directions allocated a positive value for boundary-normal flow.

The red spot is the 2014 current meter site Z, to which ABPmer flow modelling was calibrated.



2.1.2 Water Level Monitoring

Water level (tidal stage) data are recorded by the Environment Agency, from a single site in outer harbour at 15-minute intervals, and are accessed via a web-based (API) download system. These data are used in three ways:

1. Determination of low-water (LW) time and therefore enabling labelling of all data logging times in terms of hours after LW.
2. Measurement of the range (in m) of each tide (water level at HW minus level at previous LW). From these data the year can be divided into approximately twenty-five discrete neap-spring-neap cycles, each lasting about two weeks. These cycles are used to divide-up the annual time series (of turbidity and water level) in order to reveal seasonal variability in the observations.
3. Individual (15 minute) readings are used to calculate water volume changes within specific areas of the harbour (seven polygons shown in Figure 1), used in the determination of water circulation within the harbour (section 2.1.4).

2.1.3 Storm Event Monitoring

Storm events that are capable of significantly modifying water turbidity within the harbour have previously been determined³. Four basic control conditions were identified:

1. Days containing wind gust speeds >30km/hr from the north (180°) sector. These winds will create moderate wave conditions breaking along the north Wight coasts, with potential for turbid waters to be carried (under tidal or littoral drift) into the Medina estuary. These winds can also generate small amplitude waves in the outer harbour, producing erosion of mud across shallow tidal flat areas.
2. Days containing wind gust speeds >50km/hr from the south (180°) sector. These winds will create large waves in the English Channel which will break along the English coast and cause erosion of exposed seabed clay strata, tending to generate a zone of turbid water around the Wight region during the winter months³. These winds can also cause small-amplitude wave formation over the extensive shallow mudflats of the upper estuary, creating turbid water.
3. Solent Approach wave condition >1.5m Hs and 10s period. These are swell waves, not necessarily related to local storms, that can generate seabed erosion of clay strata around the south-facing shores of Wight, as described above.
4. Greater than 10mm of continuous local rainfall. Such rain will cause flooding in the rivers feeding the estuary, and influx of turbid water to the estuary. Raindrop impact can also cause bed erosion over exposed mudflats at low water during severe downpours.

Weather data is obtained from a privately run weather station near Newport, on the banks of the upper estuary, via a web-based (API) download system. The data are logged every five minutes. For each day of the year the total number of any of these four (five minute) events occurring is calculated, and this index is used to separate all the TSS data into 'storm' or 'non-storm' types.

2.1.4 Outer Harbour Water Flow Prediction.

The outer harbour has been divided into six polygons (Figure 1) for purposes of measuring fine-sediment flux. It is necessary to know the volume of water flowing across each of the polygon boundaries in order to calculate to amount of sediment moving between the polygons. Estimates are made of volume exchanges at 30-minute intervals. This information was initially derived from a



mathematical model ⁵ of tidally-driven water flow in the Medina Estuary. Such models can oversimplify the true patterns of water circulation, and to investigate the effect of this a new dataset, based on observation rather than modelling, was generated during 2019. The results of the latter study are reported fully elsewhere ⁶. Both the ‘flow modelled’ and the ‘flow observed’ datasets are used in the fine-sediment flux measurements generated for this report.

Modelled Flow. The ABPmer model runs a full spring-neap cycle simulating the two-dimensional water flow in the Medina estuary based on the period 13-29th December 2014 (full spring-neap cycle). The data from this model had been calibrated to a few recent velocity observations. The model predicts flow through each of the polygon boundaries (Figure 1) for 30-minute periods through each of the tidal cycles in the 16-day interval. Discharges were identified as positive (flowing to the east or south) or negative (flowing to west or north). The data from each profile were then sorted by tide hour and neap-rising-springs and springs-falling-neap categories, and for each half hour interval (preceding the selected tide-hour) and a 4th order polynomial curve was fitted between tide range (x) and discharge through section (y). A fuller description of the method can be found in the Ambios 2017 flux monitoring report ¹.

In initially using this methodology, potential shortcomings were identified:

1. The outer harbour in the Medina estuary contains substantially large ‘throughflow’ volumes, that is the volume passing through a polygon in a set period of time is much larger than the water volume increase in the polygon over the same period. This phenomenon is attributable to both the strong cross-flow of the Solent tide in the outer zone of the harbour, and to the formation of large gyres within the harbour (induced by the cross-flow and by recirculation against the estuary shores). The modelling results were only calibrated to a few tidal current observations in the central region of the harbour (Site Z, Figure 1, and some doppler transect data), thus leaving uncertainty that the correct amount of throughflow has been recognised in detail.
2. Because of the relatively small amount of ‘source’ data used at times of slowest flow (mostly around LW), there was significant scatter in the data points. With curve-fitting large errors were potentially occurring, particularly under conditions of ‘high spring’ and ‘low neap’ (times of few original data).
3. The latter errors introduced closure errors in the volume changes going between tidal cycles, and over the year a large amount of spurious drift occurred. This drift was removed mathematically (using a tidal-cycle running mean) that probably over-corrected the volume changes in the short-term.

Observed flow. During December 2018, a programme of current meter measurements was initiated, recording flow just above the bed over 14 day periods at sixteen sites within the outer harbour ⁶. These observations were completed by December 2019. The objective of the observations was to a) investigate the accuracy of the ABP model predictions and b) possibly identify any changes in flow patterns resulting from the February 2019 dredging of the new eastern approach channel.

The project involved two stages of analysis. Initially, 30 minute values for the north-going and east-going flow at all sites were derived, allowing harbour-wide grids of these values to be created from

⁵ Data derived from a rerun of the ABPmer model of water circulation in the Medina Estuary. ABPmer, 2015b. Cowes Local Model Calibration, ABPmer Report No R.2517

⁶ Nunny R S 2020. Tidal Circulation of Water in the Lower Medina Estuary. Report AmbCHC07 to Cowes Harbour Commissioners.



the field measurements using GIS methods, covering five groups of tidal ranges. From these, mean flow at 30 minute intervals along each polygon boundary was obtained using GIS interrogation. These data were then converted to volume changes (passing both along and normal to each polygon boundary) using further GIS evaluation of the December 2019 (latest) bathymetric survey of the harbour. The group of boundaries associated with each polygon defined a set volume-change for that polygon, resulting from the rise or fall of water over each 30 minute period. This volume was quite precisely definable from the 30 minute water-level values and December 2019 bed-level data. The second stage of the analysis involved adjusting the individual boundary flow volumes so that that the summed (volume) for each polygon equalled the true water volume change. Both a manual and an automated approach to this task were evaluated. Although the manual process can appear very objective, a clear set of rules was followed for making changes, and most of the 'observed' flow values were largely subject to only minor distortion. A few larger adjustments were necessary on boundaries ab, bc, de and hi where there was good evidence that the field observations had not correctly captured the true flow volumes. The methodology is described in detail elsewhere ⁶.

Although not fully empirical, the two-stage process described above retains the main features of the flow patterns actually observed at the sixteen measuring sites while producing a quantitative simulation of the water volume exchange that occurs between the polygons. This is thought to be an optimum way of providing the data on water volume exchange required for the fine-sediment flux quantification project. Importantly, the method did not contain residual volume values between tides, therefore no mathematical correction of 'drift' was necessary. The method therefore allows for the natural level of volume adjustment between tides to be present (infrequently showing zero volume change from LW to LW, but naturally eliminating 'drift' over longer cycles).

Comparison of the 'Modelled flow' and "Observed flow" volume exchanges between the six polygons showed broadly similar patterns, but showed significant and large quantitative differences at some localities and times. Both data sets (modelled flow and observed flow) are used (compared) in the fine sediment flux predictions.

An assumption has been made that river inflow and wind/wave effects play a subsidiary role to tidal effects in driving the WATER circulation. With river flow for example, it is known that maximum inflow, occurring for only short periods, is about $10\text{m}^3\text{ s}^{-1}$, and mean gauged river flow is of the order of $0.5\text{ m}^3\text{s}^{-1}$. These are small values compared to the average discharge⁷ value of water through the harbour entrance of $\sim 800\text{m}^3\text{s}^{-1}$. An allowance for the mean annual river flow into polygon G has been allowed for.

2.1.5 Annual Change in Harbour Bed Levels

Bed level data (bathymetry) is measured using a precision multibeam/laser system once per year (in December). Continuity of methodology is critical to enable accurate comparison of inter-annual data, and to date all surveys have been undertaken by Shoreline Surveys Ltd. A survey is made of areas along the coast in the vicinity of the harbour (polygon O, Figure 1), the outer harbour (polygons A-F, Figure 1) and the upper estuary as far south at Folly Point (part of polygon G, Figure 1).

Bathymetry measurement determines the volume change in bed levels. These data were converted, by specific locality, to dry tonnes by applying dry density values obtained from the surface 5cm of bed sediment during the 2015 survey ². In sand areas (principally outside of the harbour) a dry density of 0.9 to 1.4 t m^3 was applied to both eroding and depositing volumes, according to the 2015

⁷ Taken from the ABP model of a spring-neap cycle, with absolute values averaged.



dry density data. In predominantly mud, or gravelly mud zones values of 0.6 or 0.8 t m³ were applied, the former to depositing beds and the latter to eroding beds.

2.2 Effects of Dredging

Two dredging campaigns were undertaken in the lower Medina Estuary during 2019. Both were undertaken by Jenkins Marine Ltd, a Poole-based operator, using backhoe methods with the spoil being discharged at the Nab disposal ground. The initial survey involved the defining/deepening of the Eastern Approach Channel. It was primarily a capital dredge project, and occurred between mid-January and mid-February 2019. The second campaign followed on from the first and involved depth maintenance in Cowes Yacht Haven. This project was completed during late February/early March. After finalising the two projects, Jenkins later returned to adjust bed levels in the zone immediately south of the new offshore breakwater, completed by the end of April.

The amount (volume) of material dredged was determined by comparing pre-and post-dredge bathymetric surveys within specific local zones, and was added back to the volume-changes determined by comparing the December 2018 and December 2019 bathymetry surveys, thus effectively removing the effect of dredging and allowing the natural movement of fine sediment to be monitored. If areas dredged had deepened further by December 2019, a conversion factor of 0.8t m³ was applied to the volumes to determine the change dry sediment weight; if areas had shallowed (accumulated) the factor was 0.6 t m³.

2.3 Reconciling Flux and Bathymetry Data

The fine-sediment flux and bathymetry methods of looking at how mud circulates in the Medina estuary have their individual strengths and weaknesses:

- Bathymetry data. The total area of the outer harbour surveyed (below the chain ferry, inside the breakwater) is ~395,000m², and above the chain ferry ~481,000m², the total being 876,000m². The overall precision of standard multibeam surveys is about ±5cm. A one-centimetre slice of the whole of the bathymetry survey area contains 8,750m³ of mud, or about 7,000t of (dry) sediment at a typical bed density. Estimation of total volume changes on the estuary bed over one year are therefore imprecise unless some form of calibration can be applied to finely tune the data. Once calibrated to QC data metrics (as described in section 3.3.1), bathymetry data may show exactly WHERE sediment is accumulating/eroding but cannot say when (beyond the annual period).
- Flux data may show WHEN (on a continuous basis) bed sediment is accumulating/eroding within the six (A-F) polygons of the outer harbour, and for the whole of the estuary above section mn. This method is unlikely however to produce a particularly accurate measure of the true amounts of change involved.
- Importantly, for total change within the outer harbour area (where both methods have 100% coverage), the comparison of annual result from each method can provide a further check on the comparability of the results of the two methods, which if successful provides confidence in the total sediment budget arrived at. Reconciliation of the methods may allow the best quantitative estimates of change to be realised.

On this basis, we have compared ⁸ the fine sediment flux tonnage change and bathymetry tonnage change data and with the aim of:



1) fine-tuning the bathymetric data sediment volume changes for the whole outer harbour to QC metrics that have been developed, while at the same time ensuring they are consistent with the values determined from the flux data and

2) adjusting where necessary the end-of-year cumulative flux data within individual polygons to the annual sediment erosion/deposition volumes, as derived from the QC calibrated bathymetric data.

This analysis was undertaken for the 2016 data, with some success, and partially for the poorer quality 2017 data. Due to the poor turbidity data collection seen in 2018 the reconciliation process was not undertaken. In 2019 there was a good turbidity data recovery and a full analysis has been undertaken.

3. Results

3.1 The 2019 Total Suspended Solids (TSS) Regime.

3.1.1 Tidal Processes

Start date of cycle	01/01/2019	02/01/2019	15/01/2019	31/01/2019	14/02/2019	01/03/2019	16/03/2019	30/03/2019	14/04/2019	28/04/2019	13/05/2019	28/05/2019	11/06/2019	27/06/2019	12/07/2019	26/07/2019	10/08/2019	26/08/2019	09/09/2019	23/09/2019	08/10/2019	22/10/2019	05/11/2019	20/11/2019	05/12/2019	20/12/2019
Cycle No.	0	1	2	3	4	5	6	7	8	9	10	11	12	13	14	15	16	17	18	19	20	21	22	23	24	25

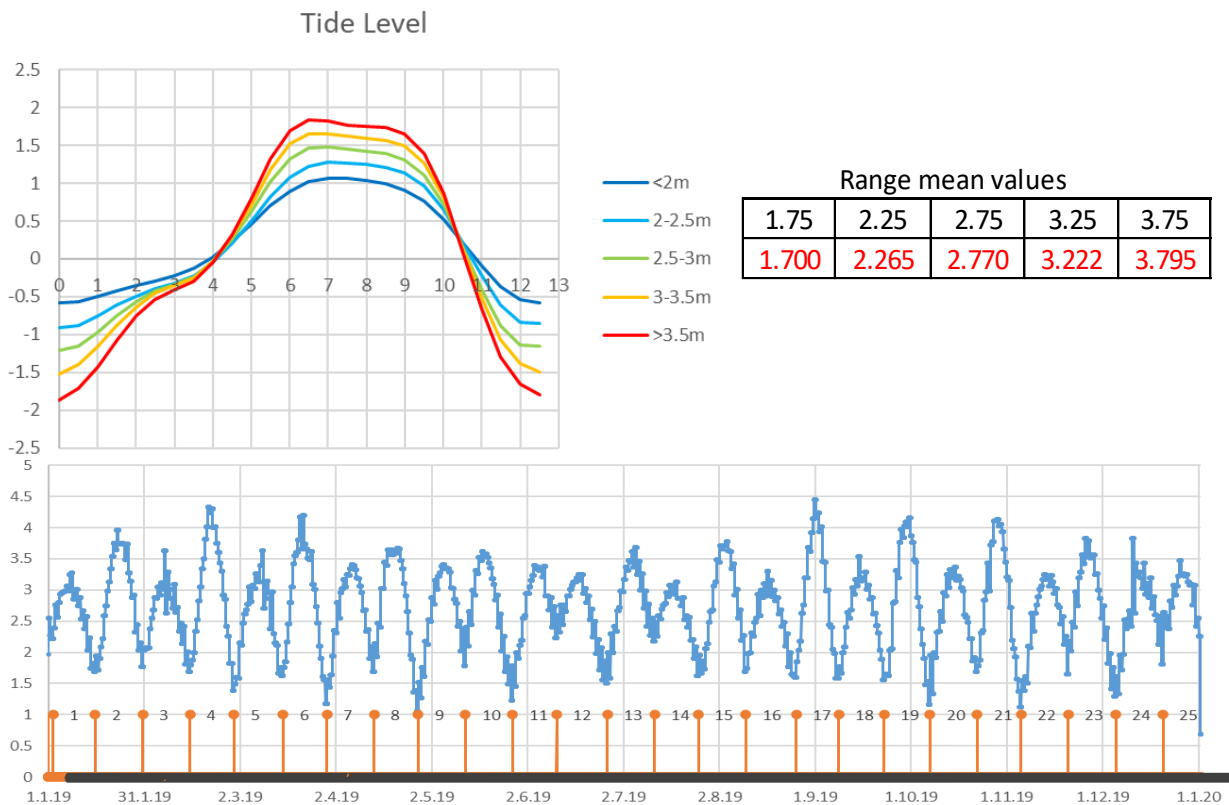


Figure 2. Tidal conditions during 2019. Top: Start dates of each of the ~25 spring-neap tidal cycles during 2019. Middle left: Average tidal cycle water levels (m CD) during 2019 within the five spring-neap tide range groups defined for the project. Middle right: Mean range values (m) for the five spring-neap tide range groups. Bottom. Graph showing the range values of individual tides through the ~25 cycles of the year.



The variability in TSS seen in the Medina estuary is thought to be to a large extent controlled by tidal processes and their associated energies, varying by tidal hour within each semi-diurnal cycle and by tidal range within the ~25 spring neap cycles through the year, the latter showing marked seasonal variability in energy levels. The range of tidal conditions prevailing in the estuary during 2019 are summarised in Figure 2, from an analysis of the 15 minute tide level data recorded in the lower Medina through that year.

3.1.2 Annual TSS Statistics

The mean values for all data recorded at all sites, of cleaned Total Suspended Solids (TSS) data per spring neap cycle⁹ for the period 2016-2019, are shown in Figure 3. It can be seen from this figure that average TSS values recorded in 2019 were much lower than in previous years, and even more so the Standard Deviation values. It is likely that much of this reduction is attributable to the successful elimination of 'biofouling' data from the records in 2019, due to the new data logging methods adopted in December 2018. The general pattern of the distribution of mean values over the four years (high concentration January-March and September-December, low concentrations through the summer months) has remained similar however.

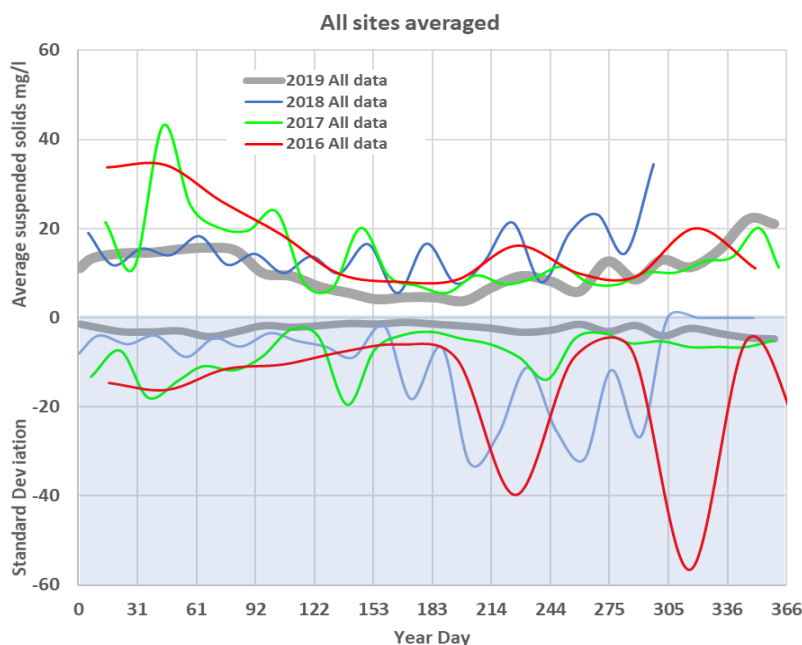
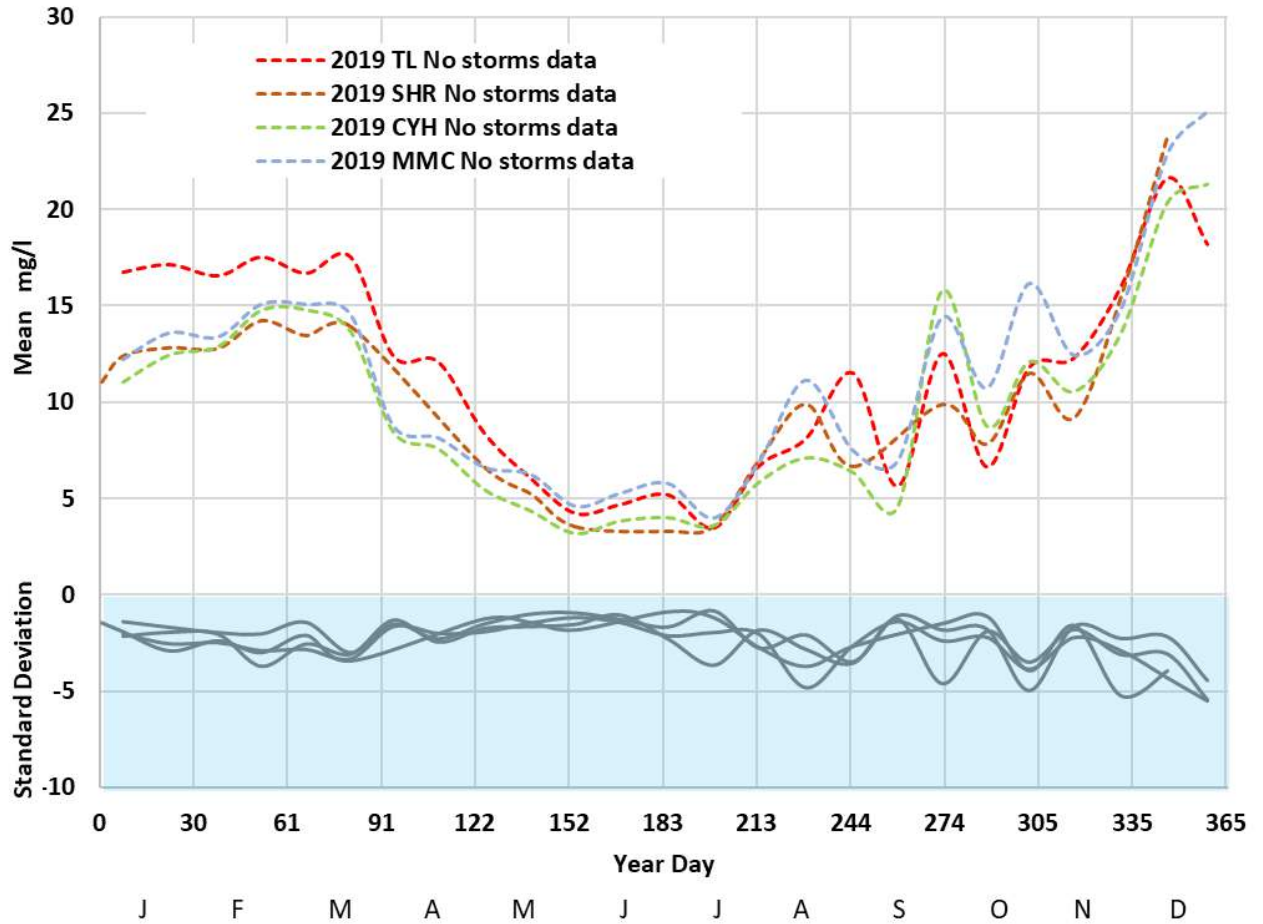


Figure 3. All TSS data combined for all sites, 2016-2019, averaged by spring-neap cycle.

The all-sites mean TSS value was 11.5 mg l⁻¹ in 2019, significantly lower than in previous years (15.1 in 2018, 14.0 in 2017 and 15.2 in 2016). It has not previously been thought useful to report this annual mean TSS concentration in the yearly monitoring reports, due to the strong suspicion (based on high summer/autumn TSS means and standard deviations) that biofouling was probably elevating the statistic above its correct value. The 2019 data probably provide the best representation yet of the TSS regime in the Medina estuary. However it is recognised that inter-annual variability naturally occurs.

⁹ Data averaged over a spring neap cycle (lowest neap to lowest neap) in 2017, 2018 and 2019. In 2016 a monthly average had been used, giving results less attuned to the controlling energies.





ANNUAL VARIABILITY IN TIDE RANGE

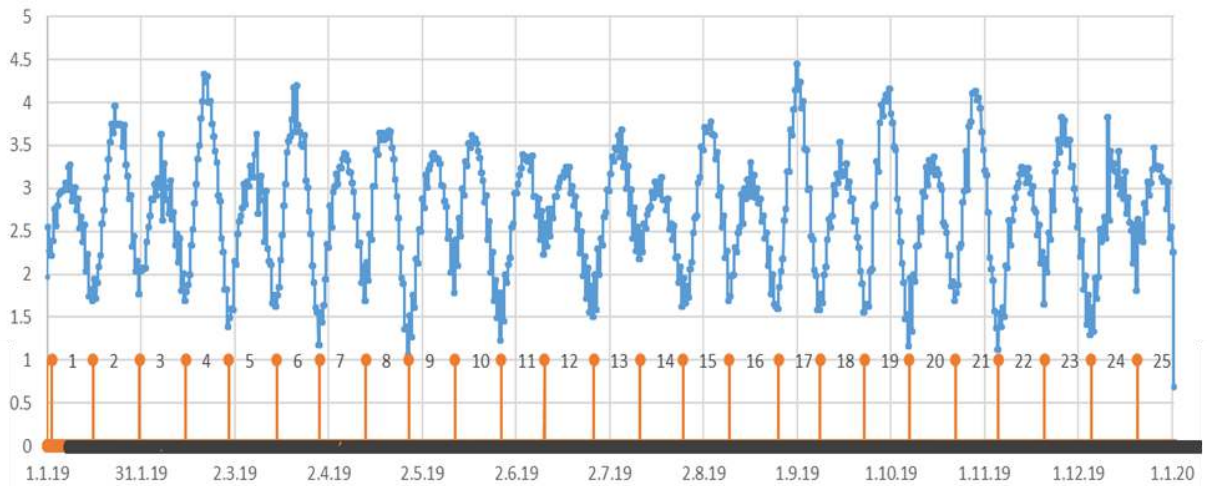
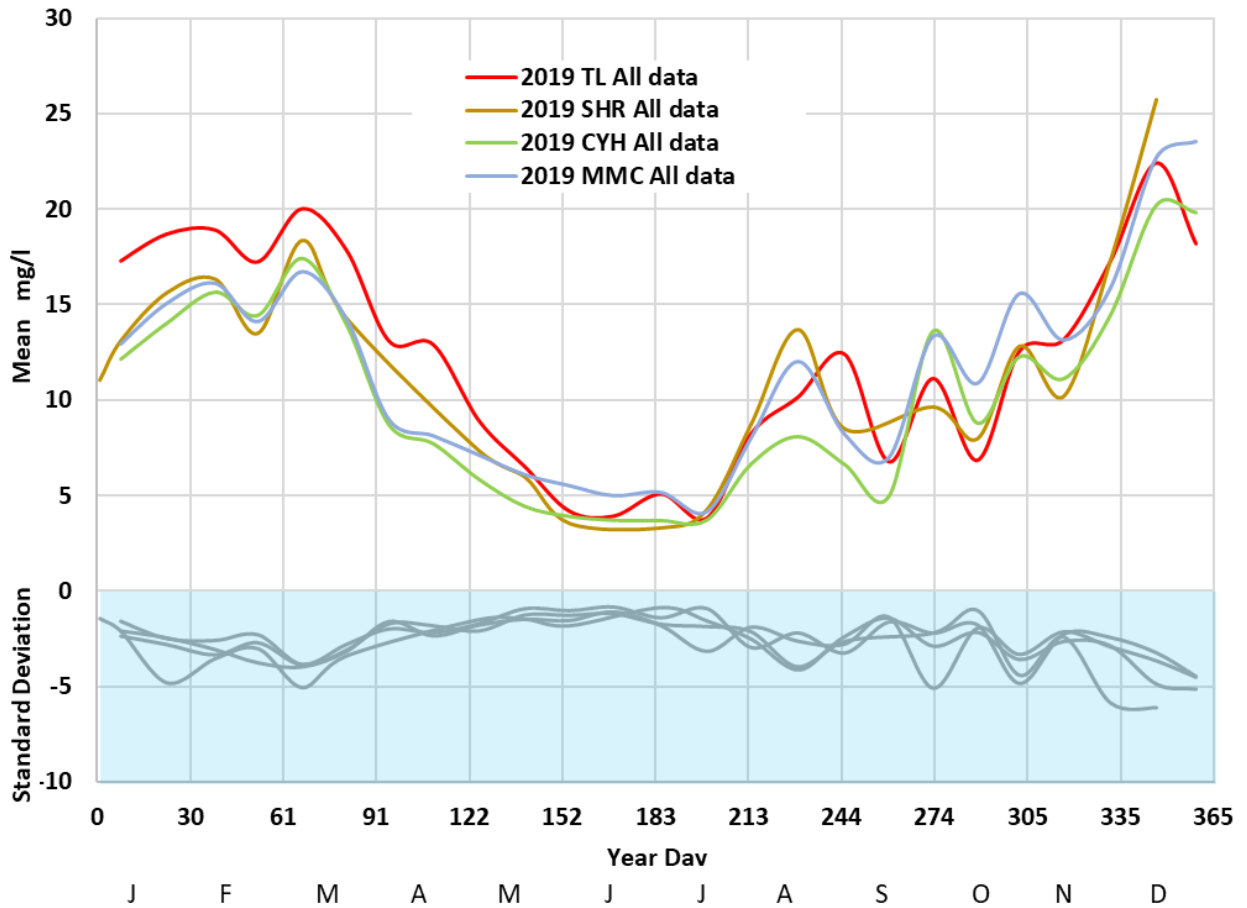


Figure 4. TSS means and standard deviations for the four monitoring sites, data with storm-days removed (top) for the ~25 spring-neap cycles through 2019 (bottom).





STORMINESS INDEX

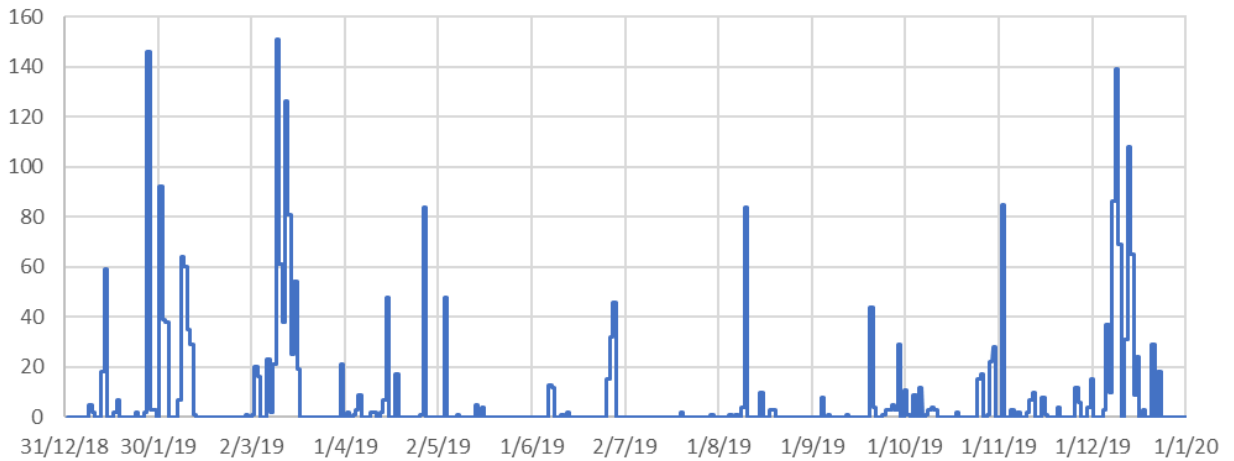


Figure 5. TSS means and standard deviations for the four monitoring sites, all data (top) for the ~25 spring-neap cycles through 2019. The annual distribution of storm events, with the number of wind/wave/rainfall events is shown below.



The all-year all-data mean TSS value (mg l^{-1}) for the four sites individually during 2019 was 11.9 (MMC), 10.6 (CYH), 11.0 (Shrape) and 12.5 (TL). These tightly cluster around the all-data mean of 11.5 mg l^{-1} . In Figure 4 the TSS mean concentrations on days with no storm event is plotted as average values for each of the ~25 spring-neap cycles through 2019. The corresponding standard deviations are plotted in the lower part of the graph. Figure 5 shows the same plot but including all data (storm days not removed). Comparison of these figures allows the following conclusions to be drawn:

- Means and standard deviations of the mean TSS values increase (but not dramatically) when storm days are included. This is consistent with observations made in previous years.
- The mean TSS concentration, but not necessarily the standard deviation, is noticeably higher through spring-neap cycles of higher peak range values and lower through those of diminished peak values, supporting the concept of tidal energy driving increased levels of fine sediment in suspension through spring tides. All the sites tend to respond equally to these cycles of increased/decreased tidal energy.
- The one period when higher TSS values did not correspond to larger tidal range (increased tidal energy) was during August (Figures 4 & 5, centred on day 230), indicating that another energy source was responsible for stirring-up fine sediment suspensions. It is possible that the peak recreational boating seen at this time of year could be responsible (Cowes Week), as observed/suggested in monitoring reports from previous years.
- There is a strong seasonal (non-tidal) change in the mean TSS levels. Mean concentrations were high ($10\text{-}20 \text{ mg l}^{-1}$) between January and March 2019, then fell steadily to a low of less than 5 mg l^{-1} by July, increasing again through the late summer, autumn, and early winter to reach maximum mean values attaining 25 mg l^{-1} . As reported initially in 2016, this seasonal pattern is likely to be driven by winter storms in the adjacent areas of the English Channel, creating a persistent region of higher TSS values around the Wight sea area from erosion of seabed clay outcrops.

The variation seen in the 'No Storm' TSS values is thought to be caused only by tidal processes, seasonal variation in regional TSS conditions, and human impacts (shipping and dredging effects). TSS values during storm-days include the effects of a range of local mud-erosion processes that temporarily and more locally elevate TSS values (section 2.1.3). The effect of these local storms upon the TSS regime is seen in Figure 6 where storm/no-storm spring-neap cycle means and standard deviations are plotted together for each of the four sites. It can be seen that all-data means can be raised by up to a maximum ~50% at times of storm occurrence, but that the standard deviations of the storm/no-storm episodes remain similar. Only at one time centred on day 274 (end of September) and at all sites (least evident at Shrape) did the 'No-storm' data means significantly rise above the 'All-data' means. The particular spring-neap cycle was one of higher tidal energy (Figure 4), and the 'storminess' index was at a low-moderate level (Figure 5). No dredging, shipping or yachting activity appears to explain this event. It is speculated that this peak might have been fed by the early autumn decay and initial breakup of the extensive brown seaweed deposits that build on East Cowes beach during the summer, and which are known to feed plumes of discoloured water into the Medina estuary as they decay.



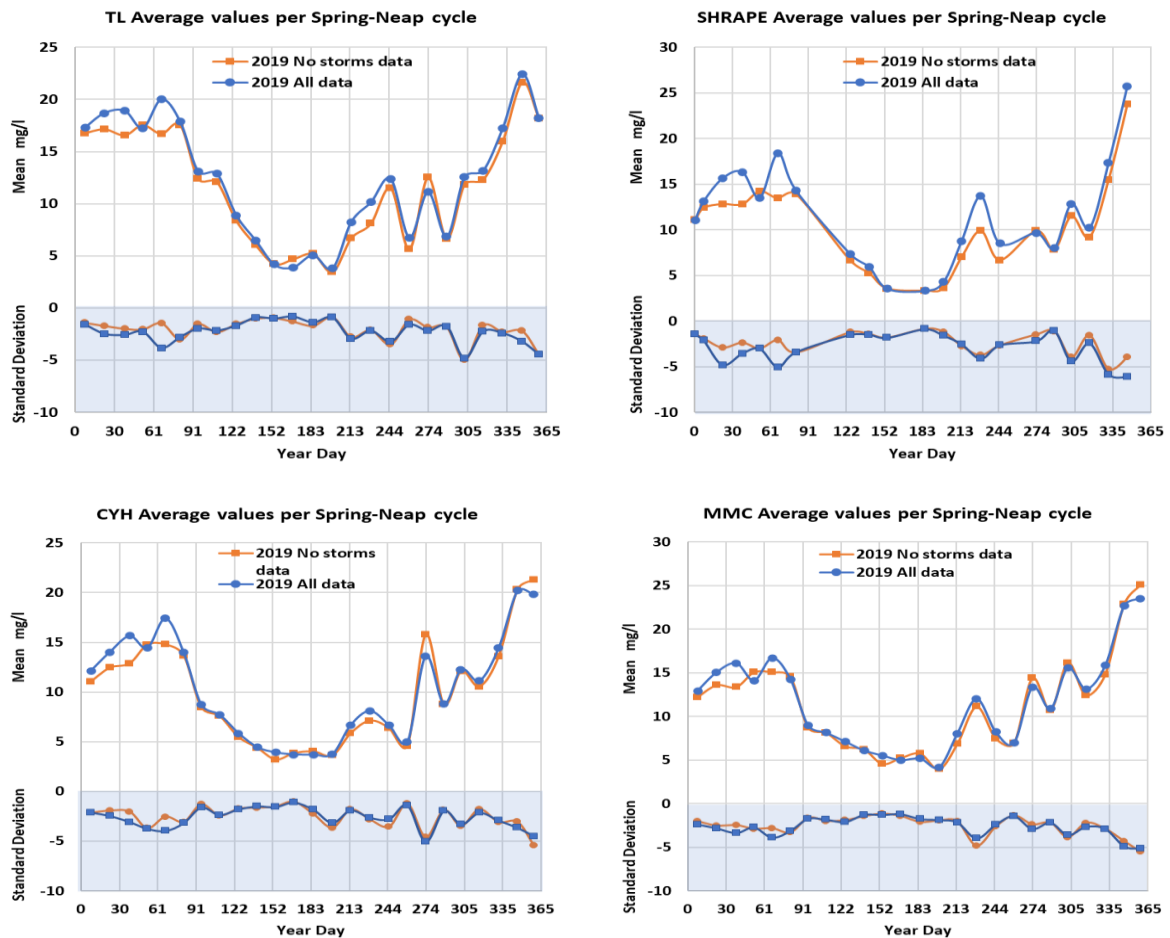


Figure 6. Means and standard deviation of TSS through the ~25 spring-neap tidal cycles of 2019, for each monitoring site individually and comparing ‘all-data’ and ‘no-storm’ data values.

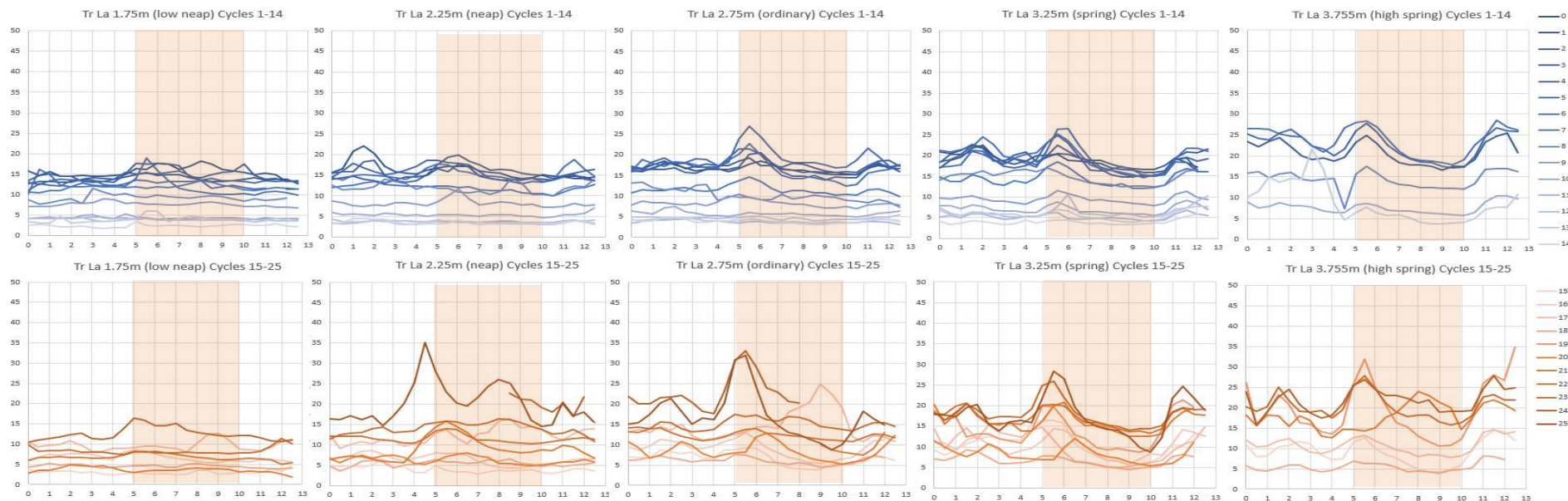
3.1.2 Tidally-Induced Variability in TSS

Figures 7-10 show, for each site and for ‘No-Storm’ conditions, the mean TSS values¹⁰ seen on each of the ~25 spring-neap tidal cycles through 2019, grouped by tidal range and plotted by tidal hour (from LW). The 25 line graphs are separated into January-July (blue) and July-December (brown) plots, and the line density varies with time between mid-winter (heavy lines) and mid-summer (light lines). The plotting technique clearly identifies the key features of the TSS distributions:

1. The seasonal change in the TSS regime, going from highest TSS concentrations in midwinter down to lowest in mid-summer (as seen in Figures 4-6). As previously mentioned, the primary processes driving this change are thought not to be local to the Medina estuary, but relate to winter storm generation of turbid water across the Solent and the adjacent English Channel region. Some local storm effects will also be present however.
2. There is a notable difference between the highest winter TSS levels of the first few months of 2019 (brown plots) and those of the last few months (blue plots). Spring-neap cycles 19,

¹⁰ Only actual data (not ‘infill’ data based on similar control conditions) have been used in deriving these figures.

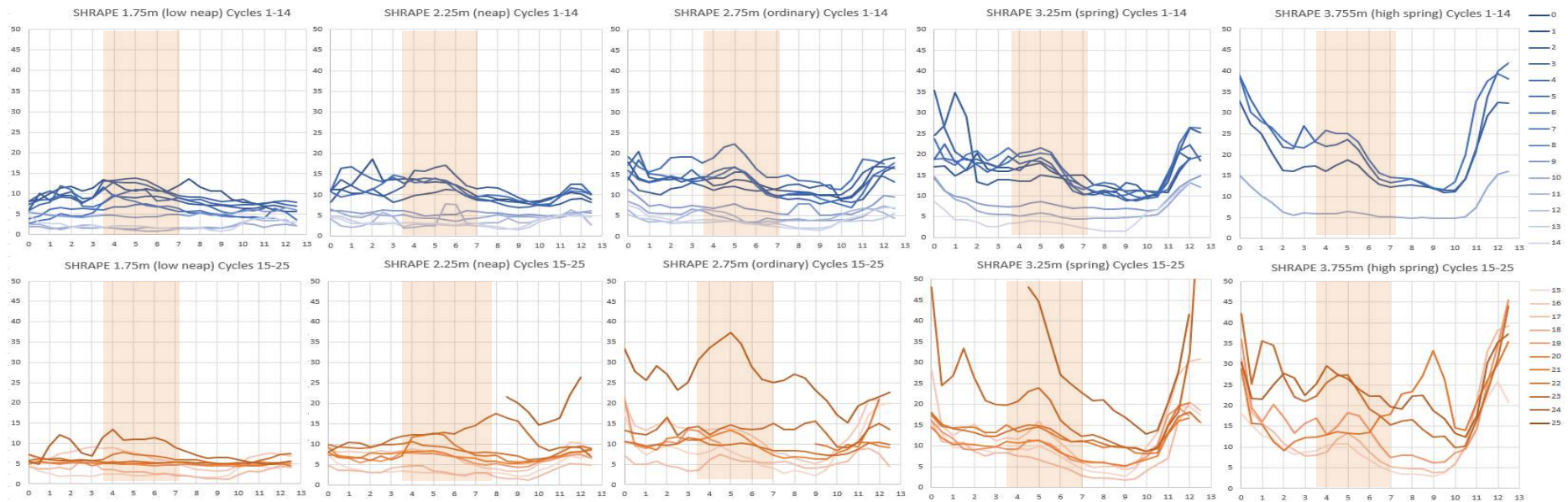




N-S cycle #	0	1	2	3	4	5	6	7	8	9	10	11	12	13	14	15	16	17	18	19	20	21	22	23	24	25
# datapoints	228	1180	1300	928	1866	350	1795	921	1321	1790	1749	1630	1724	1861	1829	1482	1712	1694	1548	239	1410	1007	1145	1432	143	1051
Year Day	1	8	23	39	53	67	82	95	110	125	140	154	169	184	199	214	229	245	259	274	288	302	316	331	346	359
<2m Range Mean	11.43	15.62	13.81	14.93	13.88	12.59	12.13	11.78	9.23	7.65	4.39	4.19	3.89	3.95	2.43	3.08	6.64	9.68	4.55	4.03	3.62	6.70	8.33	12.50		
<2m Range St Dev		0.74	1.05	1.81	1.39	0.63	3.60	1.69	0.89	1.02	0.70	0.35	0.42	0.72	0.57	1.07	3.02	4.77	0.88	0.23	1.38	4.47	1.12	1.42		
2-2.5m Range Mean	17.13	16.20	14.57	16.13	15.55		15.25	11.92	11.93	8.21	5.42	3.74	3.78	3.54	3.55	4.03	6.48	12.28	5.40		6.32	9.06	11.56	14.01	20.15	20.05
2-2.5m Range St Dev	1.35	1.00	1.12	2.34	1.54		2.30	1.40	2.88	2.13	1.02	0.91	0.78	0.70	1.04	1.44	1.46	3.96	1.34		1.65	7.40	1.62	2.02	2.48	2.84
2.5-3m Range Mean	14.17	16.70	17.02	16.86	17.06	18.98	16.66	11.52	10.21	8.19	5.74	3.79	4.70	4.06	3.96	6.70	9.10	14.64	6.15		8.43	9.15	12.32	15.09	22.83	16.97
2.5-3m Range St Dev	1.00	1.72	1.63	2.15	1.95	1.90	2.22	1.19	2.58	1.46	0.89	1.16	1.54	0.82	0.99	1.30	1.97	3.68	1.32		2.21	1.10	1.80	1.64	2.47	3.96
3-3.5m Range Mean		18.46	19.50	18.32	18.51	18.50	19.97	14.32	14.72	9.47	7.04	5.22	6.38	5.73	3.97	10.52	10.23	10.18	6.62	14.07	8.21	16.19	16.98	18.01		17.56
3-3.5m Range St Dev		2.17	2.00	1.61	1.80	1.80	2.94	1.85	2.07	1.49	1.22	1.41	2.44	1.41	0.82	6.78	1.96	2.40	1.41	1.91	1.99	2.51	2.07	3.40		6.59
>3.5m Range Mean			20.78		22.63		23.67		14.39		7.67			8.70		9.12		10.76	5.49	19.46		17.91		20.35	21.87	
>3.5m St Dev			2.70		3.33		4.00		3.06		1.25			4.79		3.27		2.62	0.55	3.40		9.47		2.94	1.61	

Figure 7. TRINITY LANDING. No-Storm data. TSS mean values (plots) by tidal hour (from LW) for each of the ~25 Spring-Neap cycles in 2019, grouped by tidal range. Each plot shows tide hour (x-axis) by mean TSS value (y-axis). Each S-N tidal cycle condition is plotted as a separate line, with the first 200 days of the year at the top (blue) and the final 165 days as the bottom (brown). Line density varies with year day (see keys on the right), lightest in mid-summer and darkest in mid-winter. The table at the bottom summarises the mean and standard deviation values for each tide range group and S-N cycle.

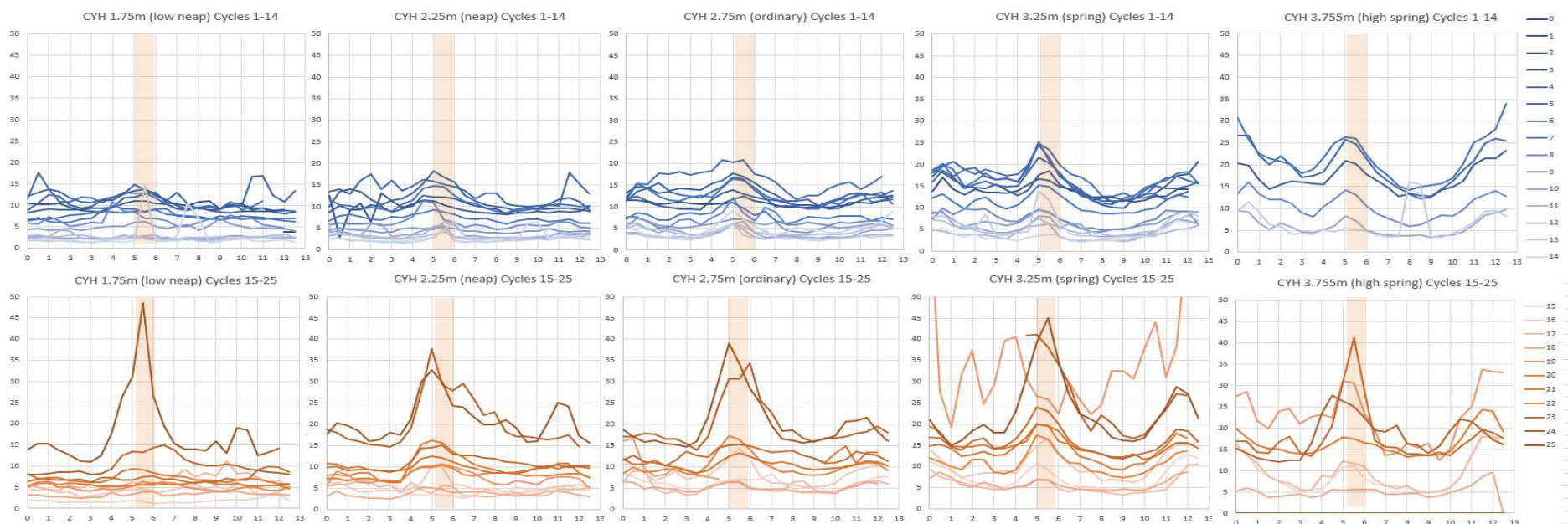




N-S cycle #	0	1	2	3	4	5	6	7	8	9	10	11	12	13	14	15	16	17	18	19	20	21	22	23	24	25
# datapoints	172	1184	1300	928	1868	350	1795	69	0	1116	1856	646	0	448	1837	1513	1712	1334	0	573	949	1001	1145	1432	341	0
Year Day	1	8	23	39	53	67	82	95	110	125	140	154	169	184	199	214	229	245	259	274	288	302	316	331	346	359
<2m Range Mean		10.20	7.96	9.78	9.13	8.00	5.69	5.52		5.02	1.86	2.02		2.37	2.76	6.48	3.15		4.85	5.00	5.98	5.73	8.16			
<2m Range St Dev		0.98	1.75	1.66	1.74	1.28	1.62	0.62		0.46	1.21	1.04		0.78	0.87	3.84	1.26		0.60	0.74	1.99	0.68	2.51			
2-2.5m Range Mean	13.49	11.42	9.23	11.83	11.37		10.74			5.58	4.83	3.89		3.21	3.40	3.89	7.07	3.38		6.36	7.15	7.90	8.68	11.63	19.37	
2-2.5m Range St Dev	2.12	1.66	1.70	2.67	2.11		3.17			1.06	1.70	2.24		0.89	1.15	1.59	2.23	0.88		0.80	1.16	4.24	1.88	4.56	2.02	
2.5-3m Range Mean	8.63	13.07	11.79	13.46	12.84	16.62	12.60			7.17	5.09	4.75		3.44	4.00	8.64	12.48	5.59		11.84	9.56	11.69	9.36	13.34	26.26	
2.5-3m Range St Dev	0.77	2.42	2.54	2.70	2.41	2.74	1.80			1.46	1.45	2.17		0.85	1.59	4.06	5.16	2.81		1.10	0.98	2.01	1.75	3.26	6.31	
3-3.5m Range Mean		14.96	16.56	16.15	15.49	15.76	17.22			8.75	6.94				4.65	9.47	13.56	7.79		10.06	9.67	12.99	12.99	21.53	25.71	
3-3.5m Range St Dev		2.59	4.76	2.49	3.17	2.27	4.31			1.97	1.41				1.24	4.00	3.65	3.38		1.43	1.58	1.93	2.02	10.76	4.06	
>3.5m Range Mean			18.62		22.33		23.41				7.56					10.36		13.50		16.33		18.96		22.82	23.80	
>3.5m St Dev			3.81		5.54		6.26				1.38					3.17		5.03		3.47		9.52		5.18	3.40	

Figure 8. SHRAPE. No-Storm data. TSS mean values (plots) by tidal hour (from LW) for each of the ~25 Spring-Neap cycles in 2019, grouped by tidal range. Each plot shows tide hour (x-axis) by mean TSS value (y-axis). Each S-N tidal cycle condition is plotted as a separate line, with the first 200 days of the year at the top (blue) and the final 165 days as the bottom (brown). Line density varies with year day (see keys on the right), lightest in mid-summer and darkest in mid-winter. The table at the bottom summarises the mean and standard deviation values for each tide range group and S-N cycle.

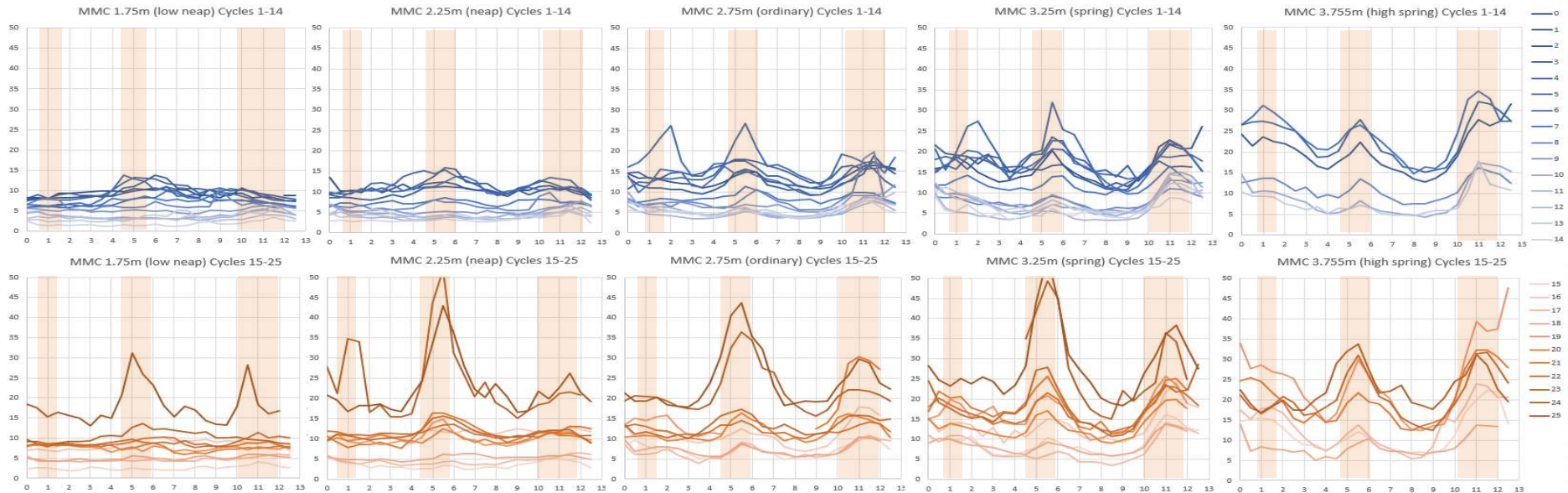




N-S cycle #	0	1	2	3	4	5	6	7	8	9	10	11	12	13	14	15	16	17	18	19	20	21	22	23	24	25
# datapoints	228	1184	1300	928	1868	350	1795	921	1352	1852	1856	1644	1852	1866	1837	1513	1712	1878	1548	575	1414	1007	1145	1432	569	1283
Year Day	1	8	23	39	53	67	82	95	110	125	140	154	169	184	199	214	229	245	259	274	288	302	316	331	346	359
<2m Range Mean	3.74	10.16	9.24	10.43	12.07	11.23	7.47	7.46	6.49	4.91	2.48	2.51	2.61	2.04	2.83	1.78	4.26	6.41	3.29	4.95	5.62	7.04	7.23	10.16	17.54	
<2m Range St Dev		0.77	1.19	1.74	4.57	1.53	1.28	0.95	1.47	1.83	0.56	0.94	0.47	0.27	3.05	0.73	3.05	4.89	0.97	0.75	1.06	2.66	1.17	1.98	3.47	
2-2.5m Range Mean	5.36	9.34	9.98	11.97	13.59		10.63	7.30	6.26	4.47	3.85	3.06	3.20	2.27	3.14	4.93	5.36	4.63	3.70	7.53	8.34	9.74	9.96	11.00	20.29	20.86
2-2.5m Range St Dev	2.61	2.32	1.46	1.96	4.41		2.27	1.01	1.50	1.30	2.34	1.20	0.82	0.92	3.10	2.09	2.88	2.94	0.90	1.17	1.81	5.22	1.66	1.97	2.77	5.62
2.5-3m Range Mean	3.80	11.00	11.05	13.43	12.68	16.15	12.35	7.94	7.03	5.69	4.14	3.38	4.35	3.20	4.97	5.99	8.35	5.50	5.04	10.02	10.27	12.64	10.60	12.70	19.68	20.11
2.5-3m Range St Dev	0.10	3.39	1.06	2.29	2.99	3.04	2.12	1.21	2.16	1.87	1.23	1.45	1.33	2.14	7.50	1.92	3.06	3.59	1.15	1.46	2.08	1.97	2.02	2.10	3.88	4.39
3-3.5m Range Mean		13.68	14.99	15.70	15.46	16.96	16.26	11.12	7.54	6.84	5.56	3.90	5.28	5.98	3.57	7.41	10.51	5.67	5.79	33.64	10.80	14.55	14.43	16.00	26.01	22.86
3-3.5m Range St Dev		2.07	3.11	2.13	2.92	3.04	3.93	2.01	2.86	1.89	2.27	2.47	1.48	4.59	0.90	1.82	2.28	1.88	2.30	12.17	2.58	2.54	2.28	3.96	3.02	6.30
>3.5m Range Mean			16.98		19.97		21.64		10.65		5.89			6.66		9.18		9.64	5.15	22.73		16.51		18.03	18.08	
>3.5m St Dev			2.83		3.59		5.73		4.20		1.77			3.44		2.50		4.37	0.86	7.44		5.01		5.43	2.13	

Figure 9. COWES YACHT HAVEN. No-Storm data. TSS mean values (plots) by tidal hour (from LW) for each of the ~25 Spring-Neap cycles in 2019, grouped by tidal range. Each plot shows tidal hour (x-axis) by mean TSS value (y-axis). Each S-N tidal cycle condition is plotted as a separate line, with the first 200 days of the year at the top (blue) and the final 165 days as the bottom (brown). Line density varies with year day (see keys on the right), lightest in mid-summer and darkest in mid-winter. The table at the bottom summarises the mean and standard deviation values for each tide range group and S-N cycle.





N-S cycle #	0	1	2	3	4	5	6	7	8	9	10	11	12	13	14	15	16	17	18	19	20	21	22	23	24	25
# datapoints	228	1184	1300	928	1868	350	1795	921	1352	1852	1856	1644	1852	1866	1837	1513	1712	1879	1548	575	1414	1007	1145	1432	569	1283
Year Day	1	8	23	39	53	67	82	95	110	125	140	154	169	184	199	214	229	245	259	274	288	302	316	331	346	359
<2m Range Mean	8.81	9.23	8.90	9.82	9.67	8.76	7.22	7.11	6.53	5.22	3.83	3.78	3.23	3.57	1.87	2.57	8.42	4.66	5.01	7.59	7.58	8.58	9.05	10.32	17.99	
<2m Range St Dev		0.75	1.55	1.52	1.32	1.07	1.60	1.05	1.06	1.03	0.80	0.94	0.80	0.90	0.68	0.94	6.18	1.21	1.02	1.68	1.33	2.58	1.17	1.60	2.85	
2-2.5m Range Mean	11.72	10.69	9.87	11.27	11.86		10.71	7.35	6.71	5.54	4.87	4.01	4.04	4.25	3.23	3.55	11.50	4.57	5.37	10.19	10.17	11.10	11.61	11.50	23.63	22.47
2-2.5m Range St Dev	1.75	1.65	1.45	2.16	2.54		2.96	1.36	1.20	1.62	1.04	0.98	1.01	2.34	1.56	1.43	6.20	1.26	0.97	1.54	1.71	4.93	1.98	2.53	6.34	4.51
2.5-3m Range Mean	9.93	13.17	12.15	15.13	13.66	17.61	13.23	8.58	8.25	7.15	5.66	4.70	5.84	5.48	5.20	7.23	11.08	6.99	7.29	13.12	11.85	22.72	12.20	13.23	21.82	24.26
2.5-3m Range St Dev	1.18	2.50	2.25	2.66	2.56	3.40	2.51	1.37	2.51	2.75	1.19	1.29	1.47	2.81	3.39	1.56	3.79	3.15	1.55	1.54	2.97	3.13	2.32	2.15	4.69	5.13
3-3.5m Range Mean		15.74	16.84	17.30	16.97	18.84	17.10	11.96	7.91	8.50	7.89	5.86	7.90	7.71	5.60	9.11	13.54	7.71	8.56	16.50	13.33	18.13	16.87	18.36	28.20	28.55
3-3.5m Range St Dev		3.15	3.46	3.56	3.46	4.02	3.82	2.73	2.13	2.24	2.00	1.46	2.41	2.72	2.14	2.88	3.10	2.86	2.05	2.82	2.76	3.75	3.36	4.42	4.47	6.90
>3.5m Range Mean			20.19		23.19		24.45		11.28		8.94			7.83		11.87		13.48	8.47	24.56		20.25		20.70	22.75	
>3.5m St Dev			3.94		4.57		5.70		3.06		2.22			1.80		3.31		4.67	1.28	4.34		4.89		3.75	3.17	

Figure 10. MMC DIVERS. No-Storm data. TSS mean values (plots) by tidal hour (from LW) for each of the ~25 Spring-Neap cycles in 2019, grouped by tidal range. Each plot shows tide hour (x-axis) by mean TSS value (y-axis). Each S-N tidal cycle condition is plotted as a separate line, with the first 200 days of the year at the top (blue) and the final 165 days as the bottom (brown). Line density varies with year day (see keys on the right), lightest in mid-summer and darkest in mid-winter. The table at the bottom summarises the mean and standard deviation values for each tide range group and S-N cycle.



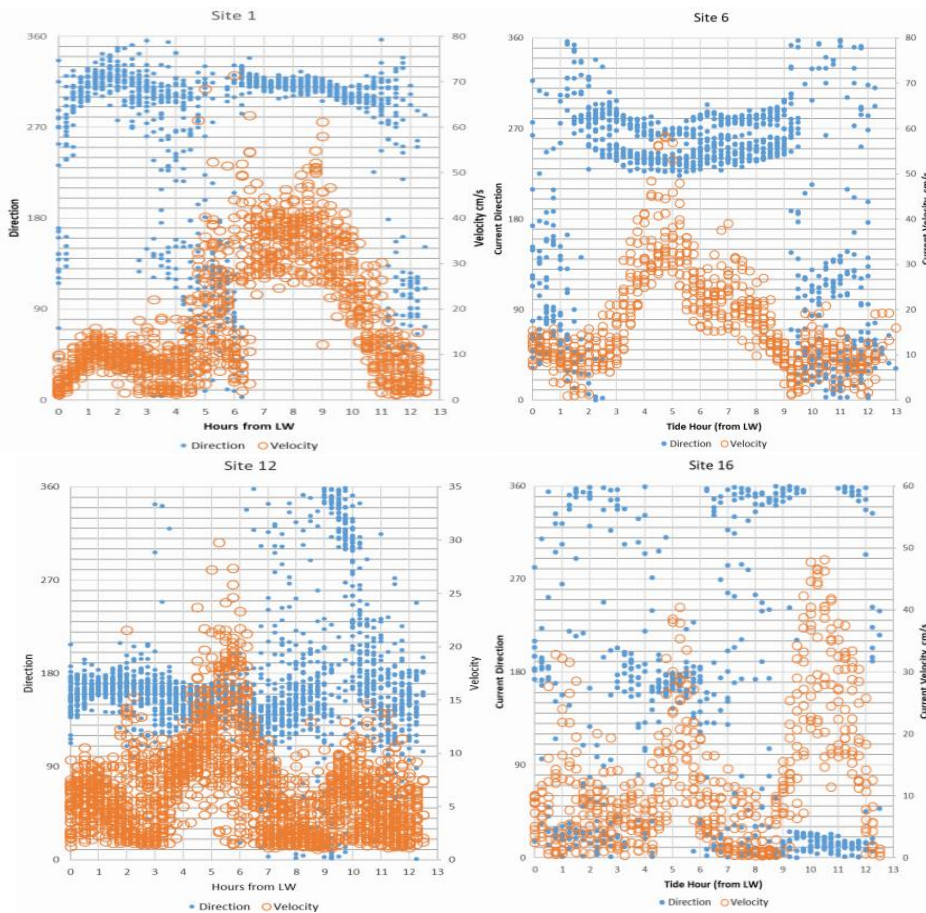


Figure 11. Data from current meter observations at Trinity Landing (Site 1), Shrape (site 6), CYH (site 12) and MMC Divers (site 16). Note difference in velocity scales (right-side y-axis).

24 and 25 in particular saw apparently abnormally high TSS values, due to the residual effect of storm conditions that occurred in the hours/day(s) preceding the plotted non-storm conditions. It will be noted later in this report (Section 3.1.4) that the occurrence of intense English Channel storms was higher in the later part of 2019 than early in the year.

3. The impact of tidal range (energy) on TSS levels (looking between the five range plots). At all sites (see table below figures) typical summer TSS values increase from 2-3mg l⁻¹ on neaps to 7-11mg l⁻¹ on springs. Midwinter values increase from ~10mg l⁻¹ on neaps to ~20mg l⁻¹ on springs. All sites seem to be equally affected by the variation in energy associated with tidal range.
4. Local resuspension by tidal currents of mud from the seabed to the water column is indicated at some of the sites. The patterns of the tidal flow at each of the four sites is shown in Figure 11 (2019 data). A velocity of 30 cm s⁻¹ is nominally taken as competent to initiate erosion of poorly consolidated mud deposits, and the approximate periods of the tide at each site when these velocities could be exceeded is shown by pink shaded areas in Figures 7-10.

The situations seen at each of the four sites varies as follows:

- Trinity Landing. The summer plots show hardly any significant variability through the tide. In the more turbid conditions earlier and later in the year a peak of concentrations typically occurs at the initiation of strong tidal flow, but does not persist through the duration of that flow. This indicates some local reworking of the muddy bed sediment, but suggests that fine sediment is in short supply, the locality therefore not being an area persistent accumulation.



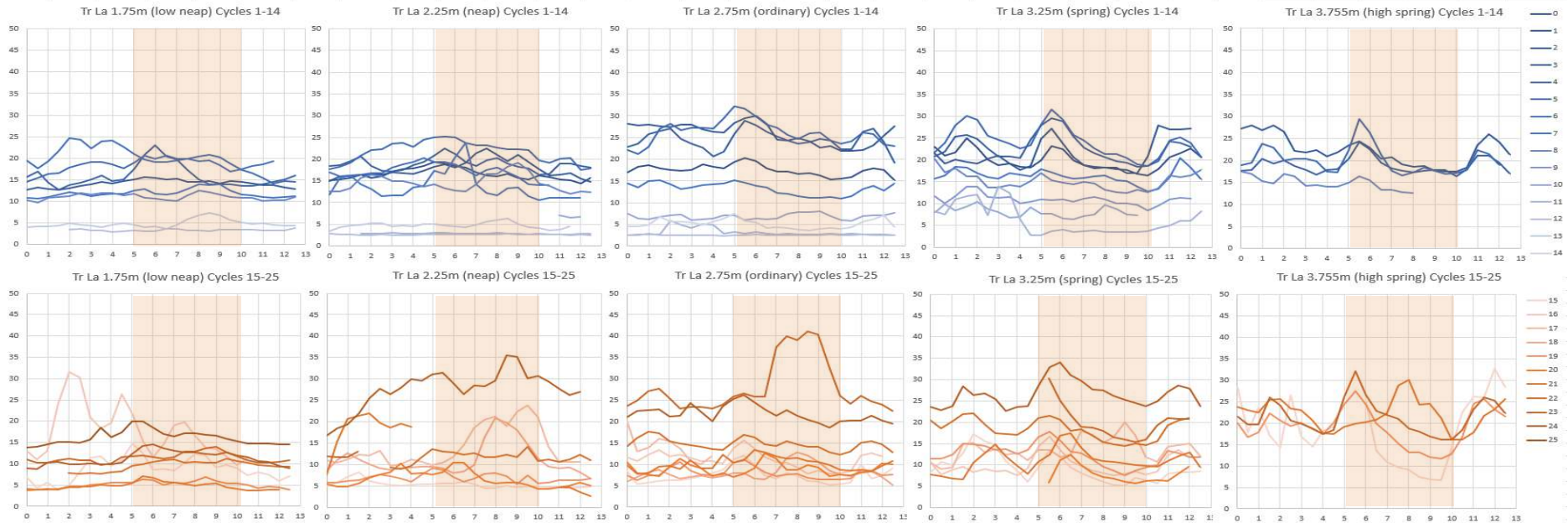
- Shrape. At low neaps through the summer there is no noticeable elevation of TSS values through the period of strongest flows, suggesting neap flows are not powerful enough to initiate local erosion. However in the winter/spring/autumn neap periods there is a definite peak in TSS values, centred on the 'strong-flow' period, showing that there is sufficient local accumulation of recently-deposited poorly consolidated mud to allow bed resuspension even under these lower tidal energy conditions. At all other (higher) tidal ranges this peak is frequently present, and strongest at times of highest tidal range and winter condition, showing the locality to be effectively if gently scoured by the tidal currents for much of the time. Other, often stronger (on the highest spring tides) TSS concentrations occur outside the period of strongest local flow, centred on the first two hours of the flood and the last three hours of the ebb. These are times of weak, recirculating local currents (Figure 11) fed, on the ebb especially, by flows coming off the shallow muddy Shrape flats inside the Shrape breakwater. Mud erosion in adjacent zones is clearly feeding the waters at the Shrape locality at these times.
- Cowes Yacht Haven. Tidal flows in this sheltered marina are much weaker than at the other sites, but the quieter conditions also create some of the least consolidated mud deposits seen in the lower estuary, thus enhancing the potential for some erosion. Peak currents only persist for an hour or two hour, on the late flood (5-6 hours after LW). On summer neap conditions no TSS peak is observed at these times, but under all other conditions some elevation of TSS concentrations coincides with the peak in tidal flow, particularly at spring tides. Very high non-storm TSS concentrations seen at this time during the latter part of the year (spring-neap cycles 19, 24 and 25) both on low neaps and high springs may indicate that higher TSS concentrations seen at this time could result from a feed of muddy water from adjacent environments associated with this short period of stronger currents, rather than erosion and reworking of the local mud bed.
- MMC Divers. There are three distinct but short-lived periods of stronger tidal currents at this site, on the early flood, late flood, and late ebb. During neap tides in the summer only the late ebb period shows some elevation of TSS values. At all other times, and particularly on high spring tides and during periods immediately following storm conditions, higher TSS concentrations are associated with these three times of stronger tidal flow, suggesting a potential for local reworking of the muddy bed in this area. The highest TSS concentrations seen at all sites occur here on the late flood during the late winter 2019 spring-neap cycles (24 & 25), higher than are seen on the late ebb currents, suggesting that these periods see strong flux of mud into the upper estuary.

The above analysis is consistent with the conclusions drawn in previous years' reports, namely that tidal energy is not the primary source of fine sediment in suspension, but plays a key role in distributing winter, Solent-derived mud into long-term sink-sites around the estuary.

3.1.3 Storm-Induced Variability in TSS.

Storm days (defined in Section 2.1.3) occurred for 33% of the year in 2019. Figures 12-15 show plots/tables of identical format to Figures 7-10, but portraying the storm-day data. In terms of the relationship between tidal currents (by tide hour and tide range) and TSS distributions, the same points made above with reference to the no-storm data generally apply; tidal energy remains a primary control of TSS distributions within semi-diurnal tidal cycles during all but the most severe storm conditions. In all cases though, the TSS average values per neap-spring tidal cycle and tide range group were, as would be expected, all higher during storm days. However the extent to which

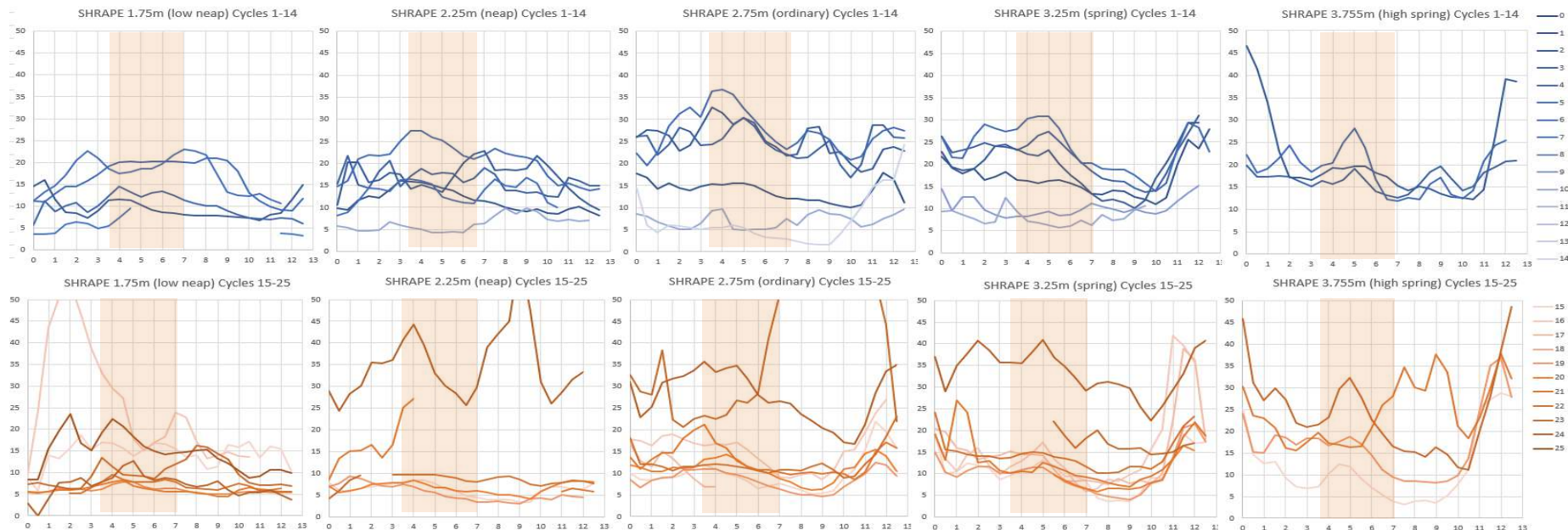




N-S cycle #	0	1	2	3	4	5	6	7	8	9	10	11	12	13	14	15	16	17	18	19	20	21	22	23	24	25
# datapoints	0	570	1233	1050	146	1787	208	1056	802	282	219	336	290	364	142	621	487	284	426	1222	560	924	1064	720	1184	0
Year Day	1	8	23	39	53	67	82	95	110	125	140	154	169	184	199	214	229	245	259	274	288	302	316	331	346	359
<2m Range Mean			14.11		15.82	17.94	20.24	11.89	11.05				3.36	4.81		8.77	17.58			5.08	4.79	9.53	11.35	11.21	16.12	
<2m Range St Dev			1.16		3.45	4.24	3.63	1.98	3.05				0.26	0.82		1.44	2.80			1.30	1.19	0.46	3.51	1.40	2.92	
2-2.5m Range Mean		16.52	17.69	18.86		21.70	17.13	13.69	14.51		6.76	2.83	2.67	4.72		5.36		14.05	11.10	6.85	6.64	13.80	11.63	12.16	27.59	
2-2.5m Range St Dev		1.37	4.84	2.24		6.03	0.86	2.59	2.78		0.27	0.15	0.15	0.50		0.92		4.05	2.14	1.67	2.16	2.69	1.05	0.77	3.57	
2.5-3m Range Mean		17.49	26.00	24.43		26.18		13.28			6.85	3.23	2.59		5.14	7.45	11.13	13.93	8.04	7.99	8.94	10.14	14.74	27.97	21.80	
2.5-3m Range St Dev		2.38	4.07	5.02		9.05		2.08			0.98	1.19	0.24		1.12	2.93	2.80	1.46	3.69	1.71	2.17	6.86	3.44	6.06	4.98	
3-3.5m Range Mean		20.04	21.21	22.88		24.18		16.30	15.16	10.98	8.11	6.25				9.36	9.90	13.67		12.44	7.82	10.98	18.38	19.87	26.56	
3-3.5m Range St Dev		1.66	3.57	4.16		4.69		3.07	1.32	2.40	1.00	1.99				2.99	1.33	2.97		2.13	1.41	3.22	3.47	1.85	4.55	
>3.5m Range Mean			22.30	18.87		20.08			14.92							18.13				19.08		22.08		21.44		
>3.5m St Dev			2.71	1.37		2.37			0.89							7.40				5.26		10.21		2.78		

Figure 12. TRINITY LANDING. Storm data. TSS mean values (plots) by tidal hour (from LW) for each of the ~25 Spring-Neap cycles in 2019, grouped by tidal range. Each plot shows tide hour (x-axis) by mean TSS value (y-axis). Each S-N tidal cycle condition is plotted as a separate line, with the first 200 days of the year at the top (blue) and the final 165 days as the bottom (brown). Line density varies with year day (see keys on the right), lightest in mid-summer and darkest in mid-winter. The table at the bottom summarises the mean and standard deviation values for each tide range group and S-N cycle.

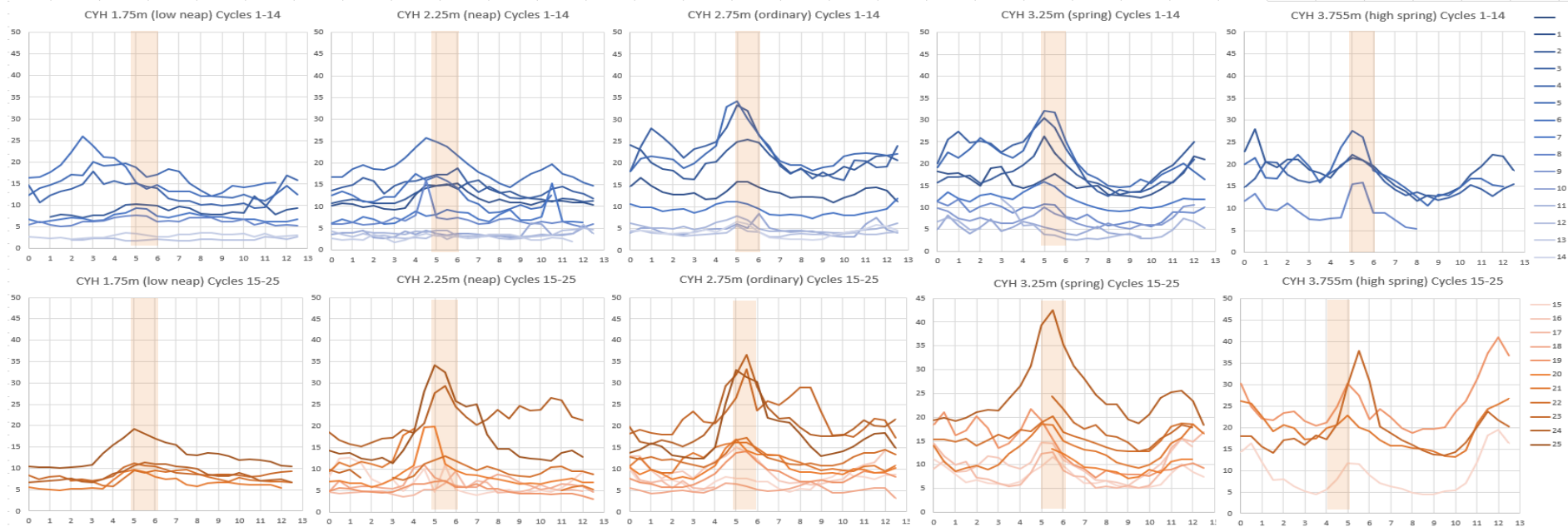




N-S cycle #	0	1	2	3	4	5	6	7	8	9	10	11	12	13	14	15	16	17	18	19	20	21	22	23	24	25
# datapoints	0	570	1086	1050	146	1787	208	1056	802	282	284	347	290	365	142	480	423	278	426	1583	560	921	1063	711	1565	287
Year Day	1	8	23	39	53	67	82	95	110	125	140	154	169	184	199	214	229	245	259	274	288	302	316	331	346	359
<2m Range Mean			9.61		9.91	16.19	17.10	5.18								14.38	25.33			5.92	6.02	6.79	9.70	6.88	14.50	
<2m Range St Dev			2.65		3.15	6.08	5.34	0.84								2.27	4.14			1.23	0.71	0.42	6.21	2.57	4.82	
2-2.5m Range Mean		11.53	16.78	16.16		20.62	13.37				6.38					6.21				5.49	6.68	13.52	8.63	7.00	35.01	
2-2.5m Range St Dev		1.38	13.02	4.29		8.33	1.32				1.10					1.48				0.93	0.99	1.93	0.48	1.18	8.17	
2.5-3m Range Mean		13.81	25.23	24.70		27.35					7.08				7.04	9.99	15.54	11.45		8.42	10.93	13.11	12.27	40.81	27.76	
2.5-3m Range St Dev		3.34	6.57	7.40		11.99					2.25				3.12	3.25	6.40	1.52		2.95	1.22	8.28	3.22	19.97	11.29	
3-3.5m Range Mean		17.01	19.30	21.92		23.68				10.21	8.03					10.55	15.50	14.65		10.30	9.01	12.95	14.41	16.93	33.63	
3-3.5m Range St Dev		2.44	4.41	5.78		5.68				2.52	1.32					2.01	3.51	3.60		2.44	0.84	2.59	3.09	3.14	8.82	
>3.5m Range Mean			21.37	16.82		18.80										11.72				16.95		24.49		24.30		
>3.5m St Dev			6.92	1.38		2.10										2.59				7.10		11.25		5.50		

Figure 13. SHRAPE. Storm data. TSS mean values (plots) by tidal hour (from LW) for each of the ~25 Spring-Neap cycles in 2019, grouped by tidal range. Each plot shows tide hour (x-axis) by mean TSS value (y-axis). Each S-N tidal cycle condition is plotted as a separate line, with the first 200 days of the year at the top (blue) and the final 165 days as the bottom (brown). Line density varies with year day (see keys on the right), lightest in mid-summer and darkest in mid-winter. The table at the bottom summarises the mean and standard deviation values for each tide range group and S-N cycle.

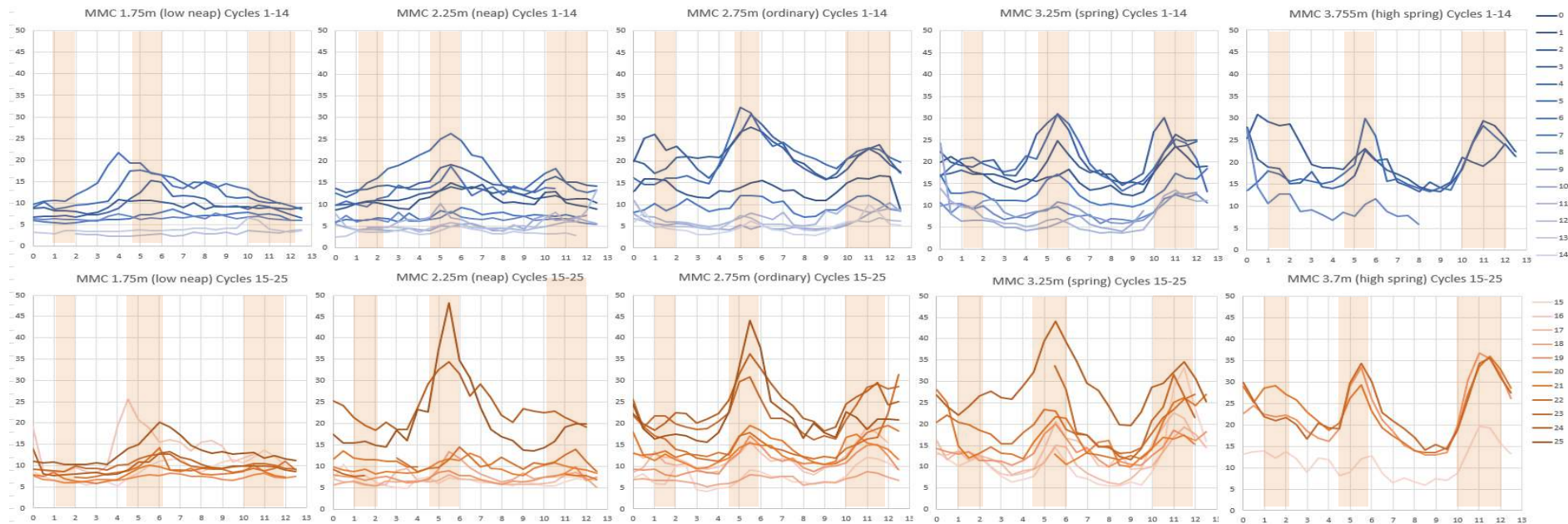




N-S cycle #	0	1	2	3	4	5	6	7	8	9	10	11	12	13	14	15	16	17	18	19	20	21	22	23	24	25
# datapoints	0	570	1086	1050	146	1787	208	1056	802	282	284	346	290	365	142	480	423	278	426	1583	560	921	1063	711	1565	287
Year Day	1	8	23	39	53	67	82	95	110	125	140	154	169	184	199	214	229	245	259	274	288	302	316	331	346	359
<2m Range Mean			8.83		12.88	15.25	16.54	7.17	6.30				2.16	2.96						5.52	6.47	7.73	8.66	8.47	13.05	
<2m Range St Dev			1.17		3.96	4.35	4.37	1.40	2.08				0.33	0.83						2.79	0.89	0.66	2.07	0.92	2.46	
2-2.5m Range Mean		11.49	12.50	14.48		18.81	12.91	7.69	6.86		3.80	3.75	4.61	2.83		7.03		5.30	6.66	5.16	8.65	10.48	9.79	9.22	21.43	17.28
2-2.5m Range St Dev		1.05	3.45	2.73		6.18	2.45	1.89	1.95		0.90	0.58	2.57	0.50		2.75		1.56	1.65	1.51	3.44	1.77	0.99	2.08	2.99	1.90
2.5-3m Range Mean		13.31	20.26	22.42		22.41		9.25			4.70	5.73	3.86		4.19	7.20	10.05	6.88	5.23	8.43	10.44	11.90	12.60	22.21	20.93	17.98
2.5-3m Range St Dev		2.63	3.54	6.64		7.04		2.04			1.68	2.10	0.70		1.18	2.10	2.65	0.95	1.75	3.52	2.30	5.45	3.08	4.12	6.75	4.24
3-3.5m Range Mean		16.07	18.00	20.70		20.86		11.82	8.81	7.37	5.14	5.17				7.46	10.06	9.11		13.00	9.82	12.84	15.75	17.30	24.80	
3-3.5m Range St Dev		2.43	2.78	4.80		4.19		2.29	1.96	2.02	1.11	2.11				1.40	1.82	2.01		7.14	1.39	2.10	3.82	2.42	5.26	
>3.5m Range Mean			18.47	16.12		17.73			9.63							9.09				25.19		19.36		19.31		
>3.5m St Dev			3.89	2.14		2.31			2.94							1.73				12.62		5.69		4.16		

Figure 14. COWES YACHT HAVEN. Storm data. TSS mean values (plots) by tidal hour (from LW) for each of the ~25 Spring-Neap cycles in 2019, grouped by tidal range. Each plot shows tide hour (x-axis) by mean TSS value (y-axis). Each S-N tidal cycle condition is plotted as a separate line, with the first 200 days of the year at the top (blue) and the final 165 days as the bottom (brown). Line density varies with year day (see keys on the right), lightest in mid-summer and darkest in mid-winter. The table at the bottom summarises the mean and standard deviation values for each tide range group and S-N cycle.





<i>N-S cycle #</i>	0	1	2	3	4	5	6	7	8	9	10	11	12	13	14	15	16	17	18	19	20	21	22	23	24	25
# datapoints	0	570	1233	1050	146	1788	208	1056	802	282	284	352	290	365	142	654	487	284	426	1583	560	924	1066	720	1574	288
Year Day	1	8	23	39	53	67	82	95	110	125	140	154	169	184	199	214	229	245	259	274	288	302	316	331	346	359
<2m Range Mean			9.17		9.34	12.09	14.08	6.76	6.55				2.96	3.84		9.00	13.94			7.14	8.01	9.16	10.04	9.76	13.02	
<2m Range St Dev			1.40		1.89	3.09	3.51	1.21	1.85				0.43	1.09		1.29	2.50			1.77	1.23	1.05	1.94	1.54	2.10	
2-2.5m Range Mean		11.06	11.86	14.87		17.34	13.06	7.34	6.59		5.11	5.66	5.57	3.57		6.59		6.80	7.51	7.36	9.70	10.26	10.92	8.29	23.78	20.67
2-2.5m Range St Dev		1.92	2.79	1.97		5.71	1.72	0.83	1.37		0.97	0.77	0.99	0.64		1.96		1.76	1.48	2.00	2.46	1.67	2.11	0.61	4.84	3.62
2.5-3m Range Mean		13.67	21.62	20.84		20.69		9.73			5.70	7.22	5.51		4.96	7.63	12.25	9.91	6.86	10.87	12.69	14.60	15.61	22.41	24.28	21.73
2.5-3m Range St Dev		3.69	4.96	6.07		6.41		2.56			0.93	1.98	1.31		1.62	2.87	3.27	2.18	1.70	3.60	2.42	5.84	3.74	4.16	8.54	5.67
3-3.5m Range Mean		17.06	18.40	21.52		20.09		13.11	8.84	9.23	6.83	7.52				11.60	13.48	11.66		13.71	13.78	17.38	18.92	20.66	28.73	
3-3.5m Range St Dev		3.00	2.51	5.96		4.31		2.79	1.37	2.88	1.01	1.64				2.88	2.85	2.14		3.82	2.58	3.23	4.67	3.09	7.01	
>3.5m Range Mean			21.69	18.21		18.36			10.59							11.34				22.44		23.56		23.32		
>3.5m St Dev			3.90	3.00		3.14			1.95							2.43				5.91		4.98		5.04		

Figure 15. MMC DIVERS. Storm data. TSS mean values (plots) by tidal hour (from LW) for each of the ~25 Spring-Neap cycles in 2019, grouped by tidal range. Each plot shows tide hour (x-axis) by mean TSS value (y-axis). Each S-N tidal cycle condition is plotted as a separate line, with the first 200 days of the year at the top (blue) and the final 165 days as the bottom (brown). Line density varies with year day (see keys on the right), lightest in mid-summer and darkest in mid-winter. The table at the bottom summarises the mean and standard deviation values for each tide range group and S-N cycle.



these TSS values were elevated on storm days (expressed as percentage increase of storm mean values over no-storm mean values) varied substantially between sites as follows:

- At Trinity Landing, on low neaps the storm values were elevated 74%. On all other tidal ranges the storm values were elevated between 15 and 26%, with no consistent variability.
- At Shrape, on low neaps the storm values were elevated 101%. This percentage elevation then decreased towards the highest tidal range (57% neaps, 63% ordinary tides, 20% spring tides, 8% high spring tides).
- At Cowes Yacht Haven, on low neaps the storm values were elevated 32%. On all other tidal ranges the storm values were elevated between 5 and 29%, with no consistent variability.
- At MMC Divers, on low neaps the storm values were elevated 26%. On all other tidal ranges the storm values were elevated between 10 and 18%, with no consistent variability.

As can be seen, the effect of storms was greatest on low neap tides, and the effects were seen most at the seaward end of the harbour and least at the boundary with the upper estuary. This observation is consistent with storm effects relating primarily to the impact of wave action, both English Channel storms raising turbidity levels in the Solent, and smaller (Solent generated) waves breaking along the shoreline at the harbour entrance and adjacent areas (including penetrating to shallow outer-harbour mudflat zones). Worst storm TSS levels were seen at Shrape during November/ December 2019, with Neap-Spring cycle means during the ebb (at nine hours after LW) attaining $\sim 60 \text{ mg l}^{-1}$ during cycle 24, and 72 mg l^{-1} during cycle 23.

3.1.4 Dredging and Shipping Impacts.

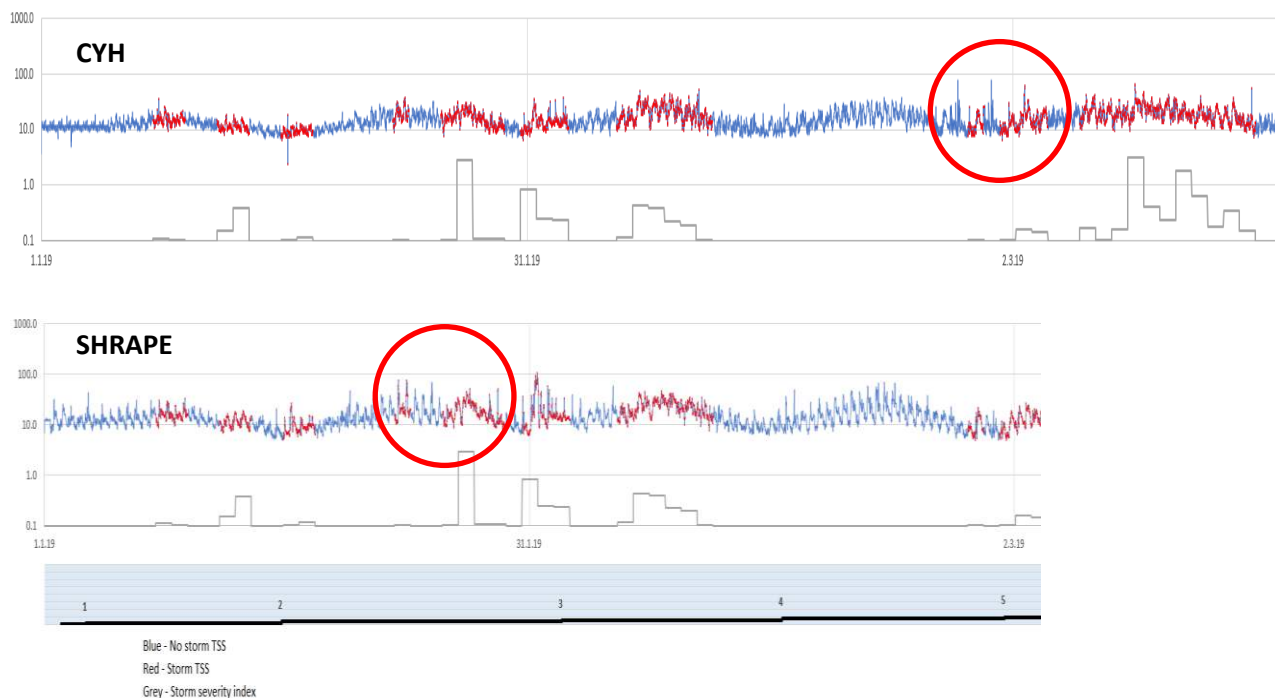


Figure 16. TSS values (15 minute averages, mg l^{-1}) logged at the two dredge sites during January and February 2019. Red circled areas identify periods when the dredger was closest to the turbidity sensors, and when individual (5 minute) TSS spikes of $\sim 200 \text{ mg l}^{-1}$ were sometimes seen. Non-storm days are blue, storm days red, with the Storminess Index shown as daily bar graphs.



The sensors at Shrape and CYH were carefully watched during the dredging period in January-March 2019. At the times when the dredger was operating close to the sensors individual (5 minute) readings attaining 200 mg l⁻¹ were occasionally seen, but these are lost during the 15 minute averaging process (values never exceeding 100 mg l⁻¹, Figure 16). The bucket-dredging methodology used appears to create no extensive plume of turbid water.

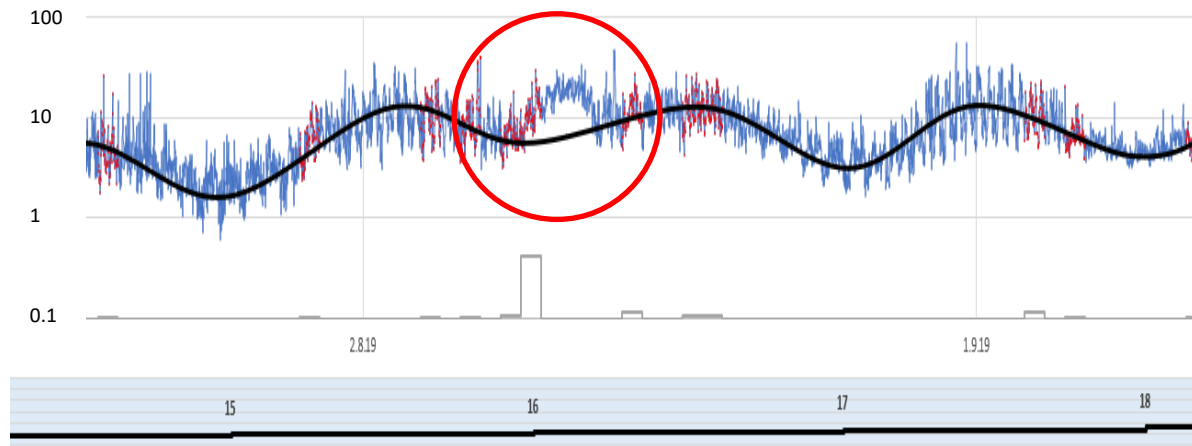


Figure 17. TSS values (15 minute averages, mg l⁻¹) logger at the MMC Divers site during late July and August 2019. The variation caused by (spring-neap) variation in tidal energy is traced as a black line. Cowes Week 2019 is circled in red.

In mid-August 2019, a peak in turbidity was observed at all sites that was not coincident with a strong spring tide (Figures 4 & 5, centred on day 230). The peak was most pronounced at the MMC Divers site. The 15 minute averaged data logged at that site is shown in Figure 17, and it can be seen that there is a period of clearly raised turbidity conditions relative to the expected variability due to tidal energy (spring -neap cycles). The coincidence of this period of raised TSS values with Cowes Week suggests possible turbidity elevation as a result of very high recreational boating activity. The impact of this type of occasional disturbance on the overall turbidity regime must be very small however.

The Red Funnel and Red Jet ferries operating into Cowes are probably the most active local shipping activities, and scouring of their turning areas at the terminals has been historically persistent. In the initial harbour monitoring report³ monthly TSS means at the four sites were compared for times of active ferry operation (6am to midnight) and for no-service periods. The analysis revealed that the no-service periods could show lower TSS values, particularly during periods of fine sediment influx from the Solent winter reservoir. This analysis has been repeated in 2019, with monthly mean values for the two periods being plotted in Figure 17. An effect was visible at all sites, least so at the MMC Divers site and most persistent at Cowes Yacht Haven, close to the Red Jet turning circle. The annual mean TSS values for the compared periods are shown in Table 2.

	CYH	TL	SHRAPE	MMC
Midnight to 6am	9.55	11.80	10.41	11.51
6am to Midnight	10.91	12.71	11.23	12.09

Table 2. Annual mean TSS values for the four monitoring sites comparing ferry operating and no-service periods.



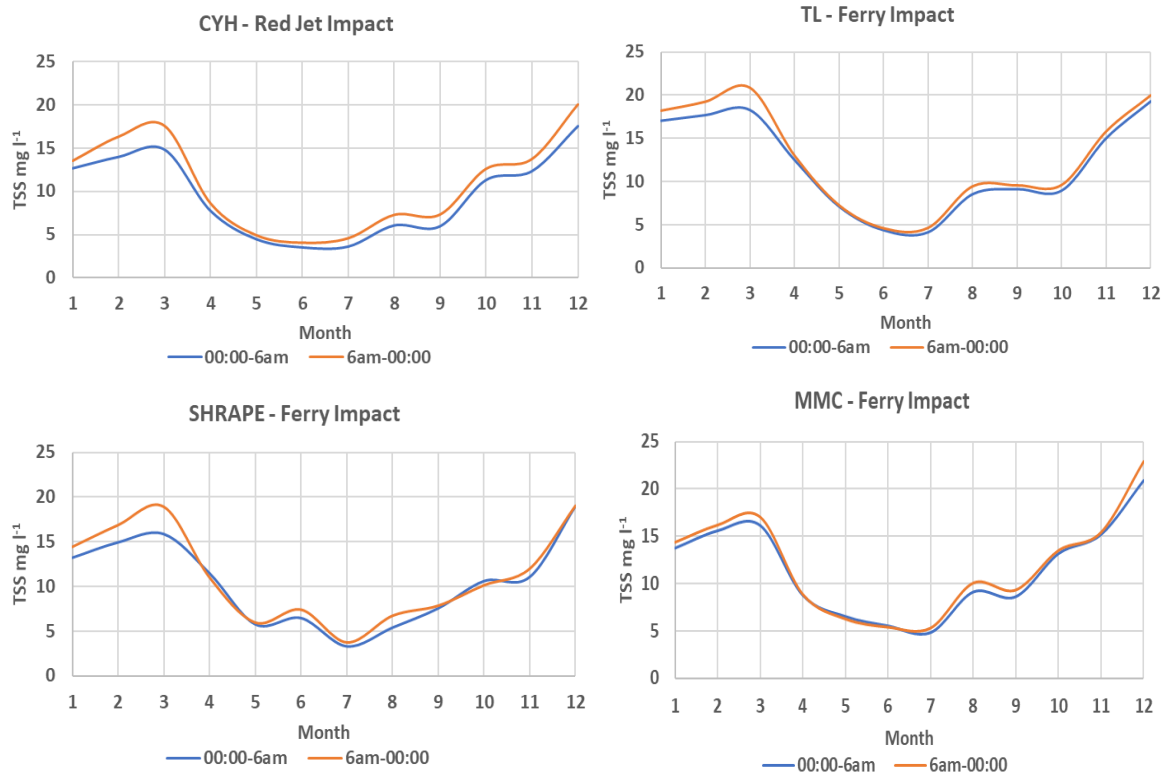


Figure 18. Monthly TSS mean values comparing ferry operating times (6am to midnight) with no-service periods (midnight to 6am).

As seen in 2016, the effect is least noticeable during periods of low supply of mud from the winter Solent-wide source (April – July), but at other times, and most persistently at CYH, the ferry-operating periods can see monthly mean values up to 3 or 4 mg l⁻¹ higher. Related to the annual average TSS figure, this is nearly the same order of magnitude as the difference between all-data and no-storm monthly means (Figure 6), supporting the 2016 report observation that shipping activity may be as-important as storms in elevating TSS values inside the harbour.

3.1.5 Inter-annual Variability

Significant inter-annual variability in the regional supply of fine sediment to the estuary has been identified as an important feature of the TSS regime. It has been speculated that this variability is driven by annual differences in English Channel storm/swell activity, creating in winter a region of more turbid water in the English Channel coastal zone around Wight (and within the Solent) as a result of increased erosion of exposed sea-bed clay strata. This process creates a large region of prolonged (winter) turbidity conditions (visible in satellite images), in contrast to the shorter-term and less widespread effects of local storm events. In seeking control variables which may represent annual variability in the winter offshore wave climate (and associated widespread turbidity generation around Wight) Sandown Bay, Milford-on-Sea and Hayling Island wave buoy data have been used. Milford represents the western approaches to the Solent, and Hayling Island and Sandown Bay the eastern approaches. A time series of the January-June ('Spring') and July-December ('autumn') recorded storm events at these sites 2003 through 2019 is plotted in Figure 16¹¹.

¹¹ Note 26% of annual observations are missing at Sandown Bay in 2018 (circled in red).



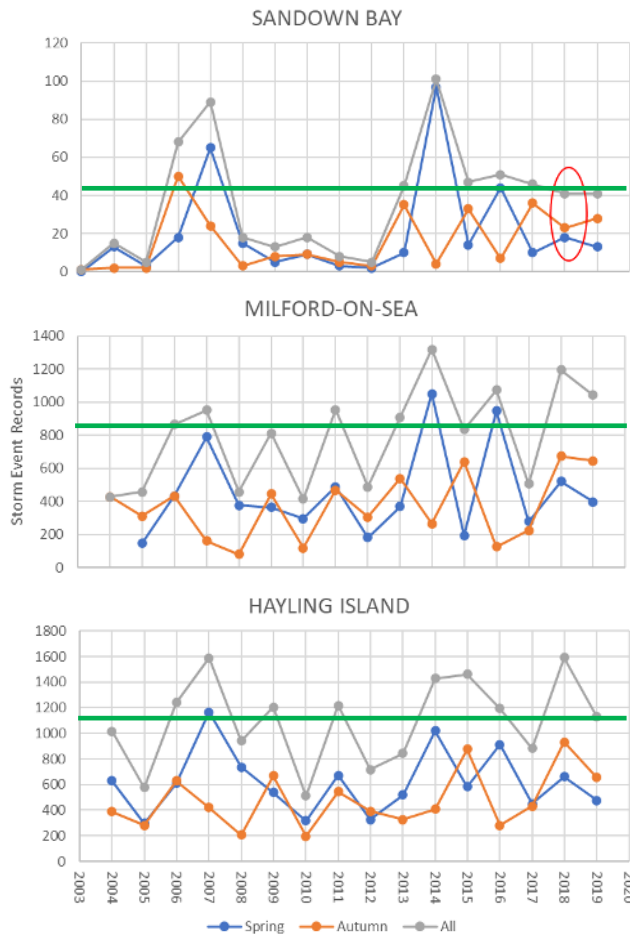


Figure 16. Frequency of occurrence of severe storms, 2003-2019, at the west Solent entrance (Milford-on-Sea), east Solent entrance (Hayling Island) and offshore (Sandown Bay) wave data buoys. Data courtesy of Channel Coastal Observatory. Buoys are located in respectively ~5m, ~9m and ~12m of water at extreme low tides. The median number of storm events over the period is shown in green.

Wave regime ‘storm events’ are defined as times when both the significant wave height exceeds 1.5m and the peak swell period exceeds 10s. It can be seen from inspecting Figure 16 that Hayling Island is subject to the largest number of such storm events each year, followed by Milford-on-Sea and then Sandown Bay. This difference is assumed to relate to the different water depths at the three sites, and the degree of shelter (from the prevailing SW waves) found in Sandown Bay.

These time series show that the inter-annual variability in storm intensiveness is marked, the total annual events varying through the period 2003-2019 between 400 and 1300 at Milford, 500 and 1600 at Hayling and 10 and 100 in Sandown Bay. 2019 saw above the annual median number of events at Milford, and around the median values at Hayling and Sandown, with more events being seen in the late year as opposed the early year at all three sites.

This seasonal (early year/late year) variability in the feed of suspended sediment to the Medina estuary in 2019 is seen clearly in the ‘All-Data’ plots of Figure 5, with the highest input seen during the English Channel stormy period of early December.

Ranking the wave-data indices for the four years that the fine sediment monitoring project in the Medina has been running, 2017 would have had the lowest winter input of mud from the English Channel source, slightly higher in 2019, higher again in 2016 and greatest in 2018.



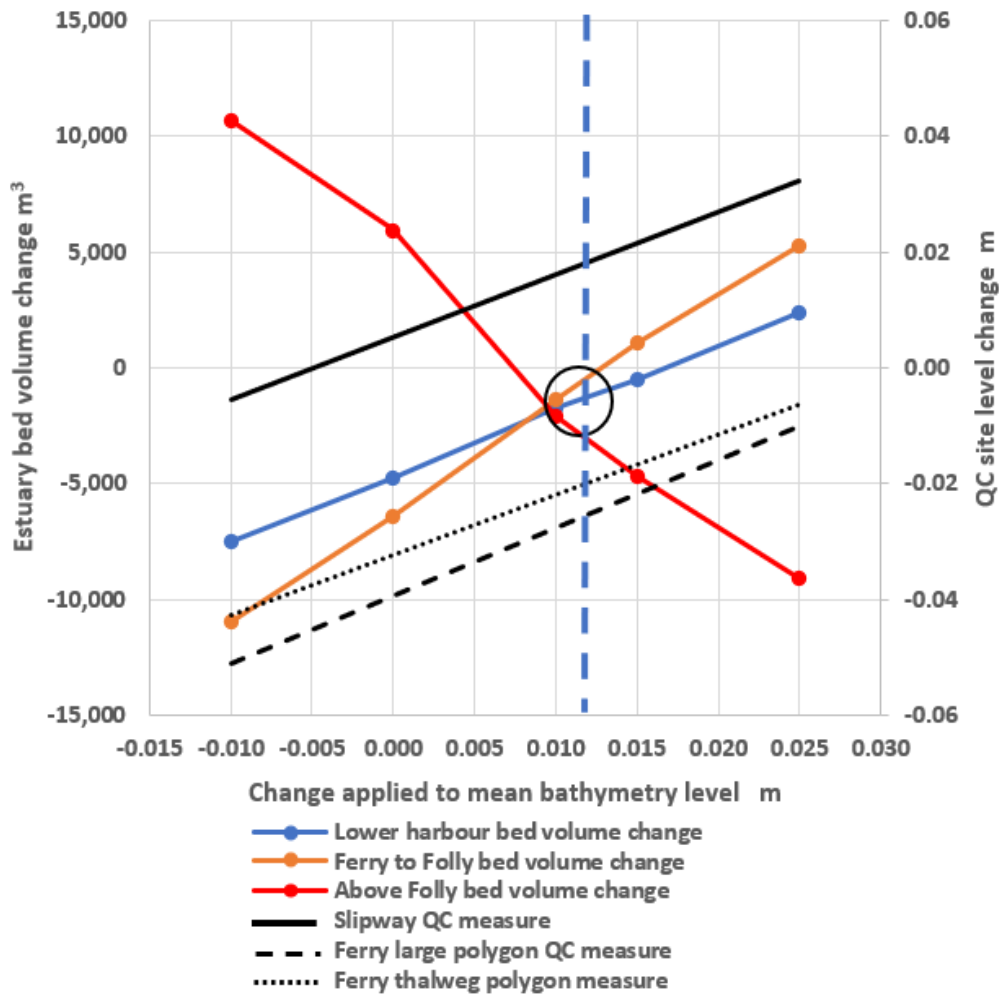


Figure 17. Summary of bathymetry mean-level adjustment values explored during analysis of the 2019 data, and estuary bed volume changes associated with each level.

The quality control data (Table 3, Figure 17) indicate that all bathymetric levels recorded during the 2019 survey should have +0.012m (12mm) added to them to be consistent with the 2015 baseline levels (making slipway and ferry thalweg QC metrics averages of +0.02 and -0.02m respectively). This compares with the -0.01m to +0.06m corrections applied in previous years (Table 2). It is noted that in the last two years this correction made to the mean level of all bathymetry measurements has been smaller than in the initial years, which may represent a real increase in precision in the survey method¹².

3.2.2 2019 Quantitative Summary

The bed volume changes from December 2018 to December 2019 has been calculated for 51 sub-polygons covering the detailed morphology of the estuary bed, as set-up in previous reports. Dredge volumes were estimated as accurately as possible from dredging records (pre- and post-dredge bed surveys), and these volumes added back into the sub-polygon datasets allowing an estimate of just

¹² “Over the past five years we have strived to continually review the accuracy of our systems. Key advances in those five years include more advanced processing techniques, greater diligence with survey methods and updating of firmware, software and hardware relating to the survey systems. The resultant product is one which is has almost halved our low error variance from around 4-6 cm to 2-4 cm.” Shoreline Surveys, May 2020.



‘natural’ changes to be presented (Appendix 2). Difficulties with interpreting accurately the dredging quantities may however have introduced some errors. Volumes were converted to dry sediment tonnage using previously identified sediment density measures (Section 2.1.5). The results were initially combined into the regions of the eight large sediment-flux polygons (A-F, G & O shown in Figure 1) plotted in Table 4. These data have been added to by information from the fine-sediment flux simulation (section 3.3) which provides a total figure for annual sediment inflow above the Chain Ferry Narrows (boundary mn), much of the upper estuary not being covered by the bathymetry surveys (which only extend to the Folly Inn). The results are shown in Table 4, together with results from previous years¹³.

ZONE	Poly	2016 <i>dry t</i>	2017 <i>dry t</i>	2018 <i>dry t</i>	2019 <i>dry t</i>
Approaches	O	4,900	3,370	5,883	20,289
Outer harbour	A	-1,536	-586	701	-329
	B	-2,629	-1,716	658	-3,253
	C	-768	-120	693	827
	D	982	72	230	1,275
	E	-2,699	-293	1,314	-388
	F	1,352	2,085	2,720	721
	Tot	-5,298	-558	6,316	-1,148
Upper Estuary to Folly	G	-3,764	3,760	1,444	-173
Above Folly		-2,030			3,859

Table 4. Historical summary of erosion and accumulation in the Medina Estuary, 1992-2019. Dredge quantities are allowed for, including capital dredge campaigns '92-'15 and in 2019. See Figure 1 for polygon locations.

In 2019 the estuary as a whole¹⁴ naturally gained ~2,600 dry tonnes of mud, after removing the effects of the volume (~62,000m³) of dredge spoil removed to the Nab Tower disposal site during the early part of the year. The outer harbour lost ~-1,100 dry t and the upper estuary (whole area above the chain ferry narrows) gained ~-3,700 dry t. Factoring in the fine-sediment flux results (Section 3.3) indicates that the latter zone saw little change in the region between the chain ferry narrows and Folly Point (~-200 dry t), and ~3,900 dry t accumulating in the reaches above this. The latter figure is derived ONLY from the sediment flux observations (section 3.3) and consequently is a less reliable figure. Over the area of the estuary above Folly (~726,000m²) the 3,900 t input equates to a net shallowing of less than 1cm.

Between 1992 and 2015 there is evidence that whole estuary naturally imported of the order of 7-10,000 dry tonnes of mud each year (based on maintenance dredging records, Appendix 2). Since 2016 (using monitoring data) we only have figures for the whole estuary for 2016 and 2019, as the bathymetry surveys do not cover the uppermost third of the estuary area and the developing fine-sediment flux project only had some success in those two years. In 2016 a loss of some 9,500 t of mud was reported, roughly equally balanced between the upper and lower estuary regions. In 2019 there was a gain of some 2,500 t of mud, principally in the uppermost region of the estuary. It is difficult to comment on these figures given the developmental nature of the fine-sediment flux work, and its limitations and programme of constant improvement of precision (sections 2.1.4, 2.3,

¹³ 2016-2018 dry tonnage data have been modified slightly from values shown in earlier reports as a result of improved handling of density data.

¹⁴ The ‘estuary’ definition excludes the harbour approaches, seawards of the breakwater, polygon ‘O’.



3.3). However the tonnages predicted for these two years are substantively lower than from the 1992-2015 evidence, suggesting that the emplacement of the new offshore breakwater in that year may have initiated a step-change (reduction) in overall rates of sedimentation within the estuary, at least temporarily. Furthermore, with the exception of 2016, the ranking of these data rates corresponds well to the English Channel storminess index (section 3.1.5, Figure 16), with 2017<2019<2016<2018. The 2016 anomaly (high erosion rates) was due to deepening in some areas (notably polygon E) which may have been due to the impact of operations during the breakwater construction.

3.2.3 Local Spatial Variability

The bathymetry-change data for the year show very clearly where erosion and deposition are occurring. These data can be seen in tabular form in Table 4, where fifty-two individual sub-polygons (small zones ¹⁵ of similar history of bed change ^{1,3}) are identified. For each sub-polygon, the annual bed level changes 2016-17¹⁶, 2017-18 and 2018-2019 are listed. The 2019 data are plotted in the three charts of Figure 18.

The key 2018 accumulation areas (>0.05m deposit, ordered by bed level change) are:

• Shepard's Wharf (5.1)	0.19m	1,595m ³	(1,130m ³ in 2018)
• West margin off Shrape Flats (9.2)	0.09m	1,610m ³	(1,260m ³ in 2018)
• East Cowes Marina Village (30.3)	0.09m	3,085m ³	(1,585m ³ in 2018)
• Red Jet Inner (8.3)	0.06m	130m ³	(100m ³ in 2018)
• West Bank south of UKSA (30.1)	0.06m	1,080m ³	(320m ³ in 2018)
• Solent Shore: West Shrape (20.1)	0.06m	3,640m ³	(sand deposition)
• South of Chain Ferry: East bank (3b)	0.06m	560m ³	(110m ³ in 2018)
• Solent Shore: East Shrape (20.3)	0.05m	2,080m ³	(sand deposition)

As can be seen, the zones of highest mud accumulation listed here showed annual volumes of accumulation little changed from 2018.

In contrast, sand accumulation outside the harbour, east of the entrance, increased strongly during 2019 (the zone showing an increase of ~16,000 dry tonnes of sand during 2019, Table 4). Increased sand accumulation within this zone was highlighted as a possible impact of the outer breakwater construction, due to modelled increases of tidal flow through the zone. Persistent sand deposition was seen in the years immediately following construction, but slight erosion was seen in 2017-18. It is likely that the impact of storm waves is dominant over tidal effects in this region, and that the latest strong build-up of sand relates to a period of storms from the NE during November-December 2019. A watching-brief should be maintained.

Erosion was marked (0.06 – 0.63m reduction in bed level) in all the ten sub-polygons where dredging occurred in 2019. Beyond these areas, >0.05m of erosion was only reported from sub-polygons 6 and 10.2, both showing clear scour areas associated with the Red Funnel ferry operations (Figure 18). Interestingly, the Red Jet turning site (8.4) which has shown scouring since 2015 was stable in 2019, suggesting the scour pit may now have developed to an equilibrium geometry (although deposition persists across the bank along its inshore margin (8.3, Figure 18).

¹⁵ Note these zones and the flux polygons are not exactly contiguous, explaining some minor level of discrepancy between values derived from analyses based on one geometry or the other.

¹⁶ Data for earlier years can be seen in the 2018 sediment monitoring report.



poly	Site Description	Area m ²	2016-17 m ³	Continuity 16-17 times	Level change 2016-17 cm	Volume by zone m ³	Plus dredge removal m ³	2017-18 m ³	Continuity 17-18 times	Level change 2017-18 cm	Volume by zone m ³	2018-19 m ³	Continuity 18-19 times	Level change 2018-19 cm	Volume by zone m ³	Plus dredge removal m ³	
	17.1 Coast slope north of breakwater	70,772	70	0.0	0.1			3,212	45.9	4.5		-5,056	-1.6	-7.1		8,705	
	17.3 Coast slope eastern sector	25,891	227	-5.5	0.9			772	3.4	3.0		943	1.2	3.6			
	19b East Harbour Entrance	40,949	-489	0.6	-1.2			-377	0.8	-0.9		-4,429	11.7	-10.8		5,421	
	12 Shrape Breakwater zone	12,492	-348	-0.3	-2.8			837	-2.4	6.7		474	0.6	3.8		m3 dredged	Harbour Approaches (outside new breakwater)
	20.1 Solent shore: West Shrape	59,892	1,463	-38.5	2.4			-1,146	-0.8	-1.9		3,643	-3.2	6.1			
	20.2 Solent shore: Mid Shrape	83,360	1,451	3.3	1.7			-98	-0.1	-0.1		4,106	-41.9	4.9			
	20.3 Solent shore: East Shrape	40,663	103	0.1	0.3		No dredging	180	1.7	0.4		2,076	11.5	5.1			
	21.1 Main Fairway entrance	5,032	-61	4.1	-1.2			46	-0.8	0.9		125	2.7	2.5			
	21.2 West of entrance Solent shore	6,910	-7	0.0	-0.1	2,409	2,409	251	-35.9	3.6	3,677	79	0.3	1.1	1,959		16,085 OPEN COAST
	14.1 West side of Fairway entrance	18,126	-265	0.3	-1.5		2,057	445	-1.7	2.5		-714	-1.6	-3.9		No dredging	
	14.2 Trinity Landing & RYS	12,712	-2,225	2225.0	-17.5		m3 dredged	638	-0.3	5.0		441	0.7	3.5			-138
	15 West thalweg, inner entrance	7,784	-206	0.4	-2.6	-2,696	-639	86	-0.4	1.1	1,169	135	1.6	1.7	-138		POLYGON A
	17.2 Eastern fairway sideslope	5,338	-230	1.5	-4.3			-95	0.4	-1.8		101	-1.1	1.9		m3 dredged	
	18a Outer harbour mid-zone	41,299	-369	0.4	-0.9			889	-2.4	2.2		-11,090	-12.5	-26.9		7,593	
	16 East thalweg, inner entrance	7,616	-92	1.8	-1.2		No dredging	175	-1.9	2.3		291	1.7	3.8			
	8.1a Fairway off West Cowes	20,792	-499	1.0	-2.4		dredging	366	-0.7	1.8		-1,333	-3.6	-6.4		1,665	-4,200
	19a East Harbour Entrance	17,611	-688	0.8	-3.9	-1,878	-1,878	-127	0.2	-0.7	1,208	-6,461	50.9	-36.7	-18,491	5,033	POLYGON B
	14.3 West Cowes shore private area	8,244	256	-3.2	3.1			531	2.1	6.4		377	0.7	4.6			
	8.1b Fairway off West Cowes	14,330	-113	0.2	-0.8			164	-1.5	1.1		487	3.0	3.4			
	8.2 Shore off Fountain Quay	7,876	-465	42.3	-5.9		1,636	439	-0.9	5.6		362	0.8	4.6		No dredging	
	8.3 Red Jet inner	2,116	-854	-16.7	-40.4		m3 dredged	92	-0.1	4.3		133	1.4	6.3			1,378
	8.4 Red Jet outer	1,920	-437	1.6	-22.8	-1,613	23	-47	0.1	-2.4	1,179	19	-0.4	1.0		1,378	POLYGON C
	18b Outer harbour mid-zone	16,709	-174	0.4	-1.0			292	-1.7	1.7		-2,389	-8.2	-14.3		2,591	
	9.1 Venture Quay and Small Boat Channel	27,461	-548	0.9	-2.0			496	-0.9	1.8		-101	-0.2	-0.4		m3 dredged	
	9.2 West margin off Shrape Flats	17,300	573	0.3	3.3		No dredging	1,262	2.2	7.3		1,610	1.3	9.3			
	10.1 Outer Shrape Flats	11,993	217	0.4	1.8			-155	-0.7	-1.3		101	-0.7	0.8			2,193
	11 Inner Shrape Flats	34,196	76	0.1	0.2	144	144	-956	-12.6	-2.8	939	381	-0.4	1.1	-399		POLYGON D
	8.1c Fairway off West Cowes	35,126	-1,016	0.5	-2.9			89	-0.1	0.3		-2,860	-32.1	-8.1		3,168	
	5.1 Shepard's Wharf	8,228	-4,291	-4.8	-52.2			1,129	-0.3	13.7		1,595	1.4	19.4		m3 dredged	
	5.2 Fairway off Shepard's Wharf	4,358	-1,999	66.6	-45.9			166	-0.1	3.8		183	1.1	4.2			Outer Harbour (inside new breakwater)
	5.3 Fairway south of Shepard's Wharf	8,068	-361	1.1	-4.5			190	-0.5	2.4		253	1.3	3.1			
	6 Fairway off Car Ferry Terminal	11,261	-228	0.3	-2.0			64	-0.3	0.6		-2,326	-36.3	-20.7			
	7 Car Ferry Terminal	4,928	-33	0.1	-0.7			-29	0.9	-0.6		212	-7.3	4.3			
	10.2 Embayment off Maritime Museum	2,576	-21	-0.4	-0.8			121	-5.8	4.7		-457	-3.8	-17.7			
	4 Fairway north of Chain Ferry	4,958	-58	0.3	-1.2		7,378	129	-2.2	2.6		117	0.9	2.3			
	2a North of Chain Ferry west bank	8,430	-26	0.1	-0.3		m3 dredged	135	-5.2	1.6		312	2.3	3.7			332
	3a North of Chain Ferry east bank	9,700	-171	0.5	-1.8	-8,204	-826	211	-1.2	2.2	2,205	136	0.6	1.4	-2,837		POLYGON E
	13.1 CYH north	8,204	303	0.7	3.7		1,064	1,301	4.3	15.9		-4,423	-3.4	-53.9		6,190	
	13.2 CYH south	13,764	1,435	0.7	10.4		m3 dredged	2,823	2.0	20.5		-8,714	-3.1	-63.3		9,473	1,849
	13.3 Corinthian YC	4,320	-972	-3.8	-22.5	766	1,830	409	-0.4	9.5	4,533	-678	-1.7	-15.7	-13,815	m3 dredged	POLYGON F
	1 South of Chain Ferry channel centre	17,639	-268	0.4	-1.5			265	-1.0	1.5		496	1.9	2.8			
	2b South of Chain Ferry west bank	18,536	-487	2.2	-2.6			615	-1.3	3.3		837	1.4	4.5			
	3b South of Chain Ferry east bank	9,874	56	-1.2	0.6			107	1.9	1.1		555	5.2	5.6			
	30.1 West bank south of UKSA	17,408	129	0.2	0.7			320	2.5	1.8		1,076	3.4	6.2			
	30.2 Channel off East Cowes Marina Village	61,493	-781	1.0	-1.3			981	-1.3	1.6		1,263	1.3	2.1			Upper estuary (above chain ferry to Folly Inn)
	30.3 East Cowes Marina Village	35,736	3,654	-0.3	10.2			1,574	0.4	4.4		3,086	2.0	8.6			
	30.4 Medina Wharf	10,596	-264	0.9	-2.5		414	457	-1.7	4.3		177	0.4	1.7			
	31 Estuary off Kingston Wharf	70,069	-174	0.1	-0.2		m3 dredged	1,114	-6.4	1.6		-424	-0.4	-0.6			
	32 Upper estuary to Folly Inn	230,627	2,447	-0.5	1.1	4,312	4,726	-2,018	-0.8	-0.9	3,415	2,990	-1.5	1.3		No dredging	
	31a West bank mid-estuary intertidal	102,900										-3,017		-2.9		2,404	2,404
	31b East bank mid-estuary intertidal	99,750										-4,634		-4.6	2,404		POLYGON G
	33 Above Folly	726,000															Above Folly Inn



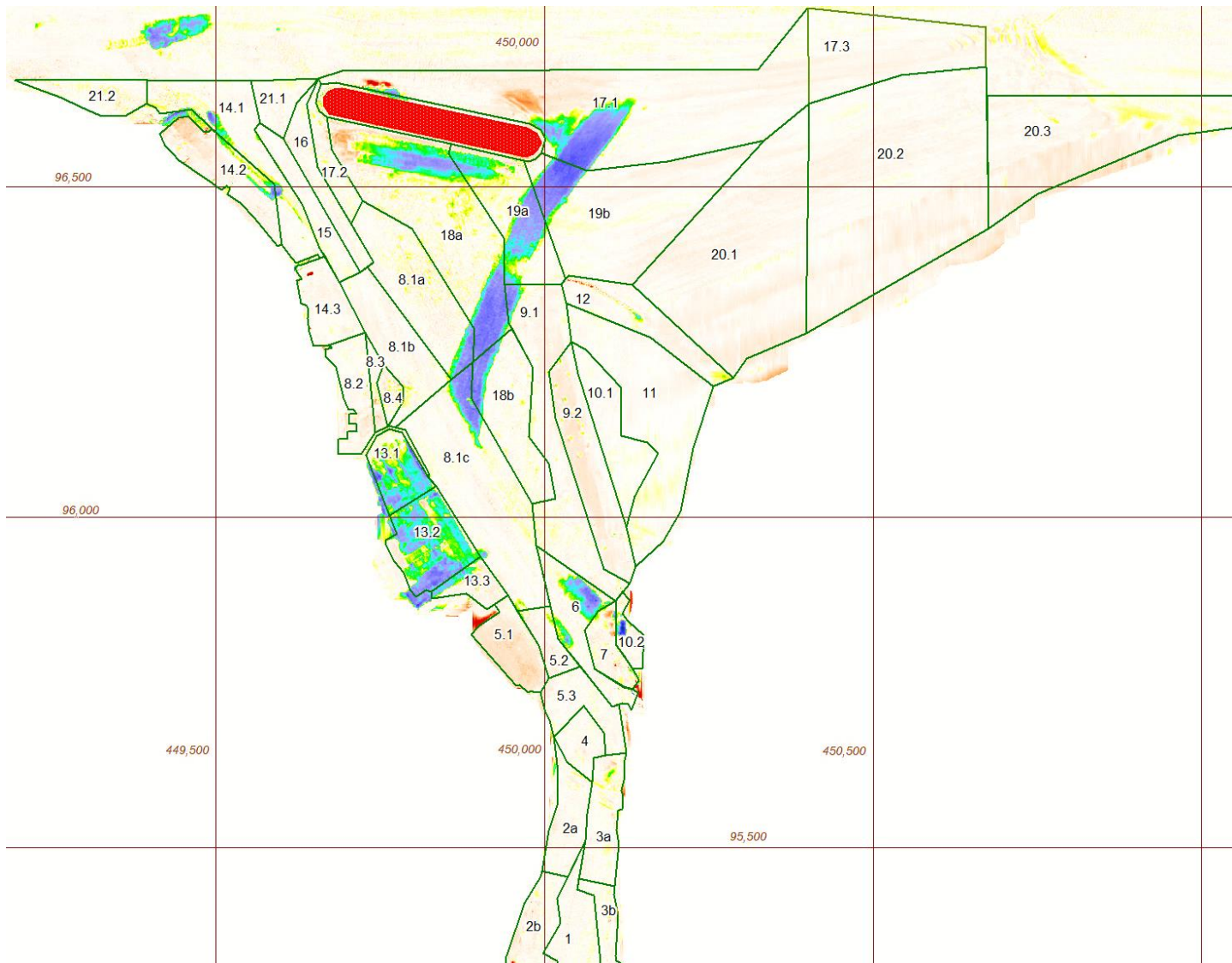


Table 5. (Previous page) Bed level changes between December 2016, December 2017 and December 2018, by estuary zone (see Figure 18 for zone location). The continuity index compares volume change with the previous year.

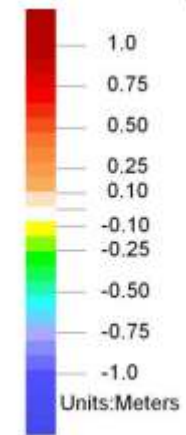
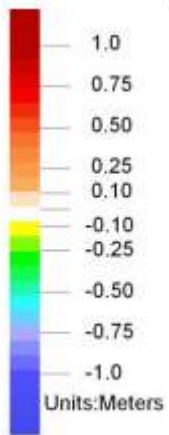


Figure 18 (left and over page). Chart showing change in bed levels from December 2017 to December 2018 (left and continues overleaf).





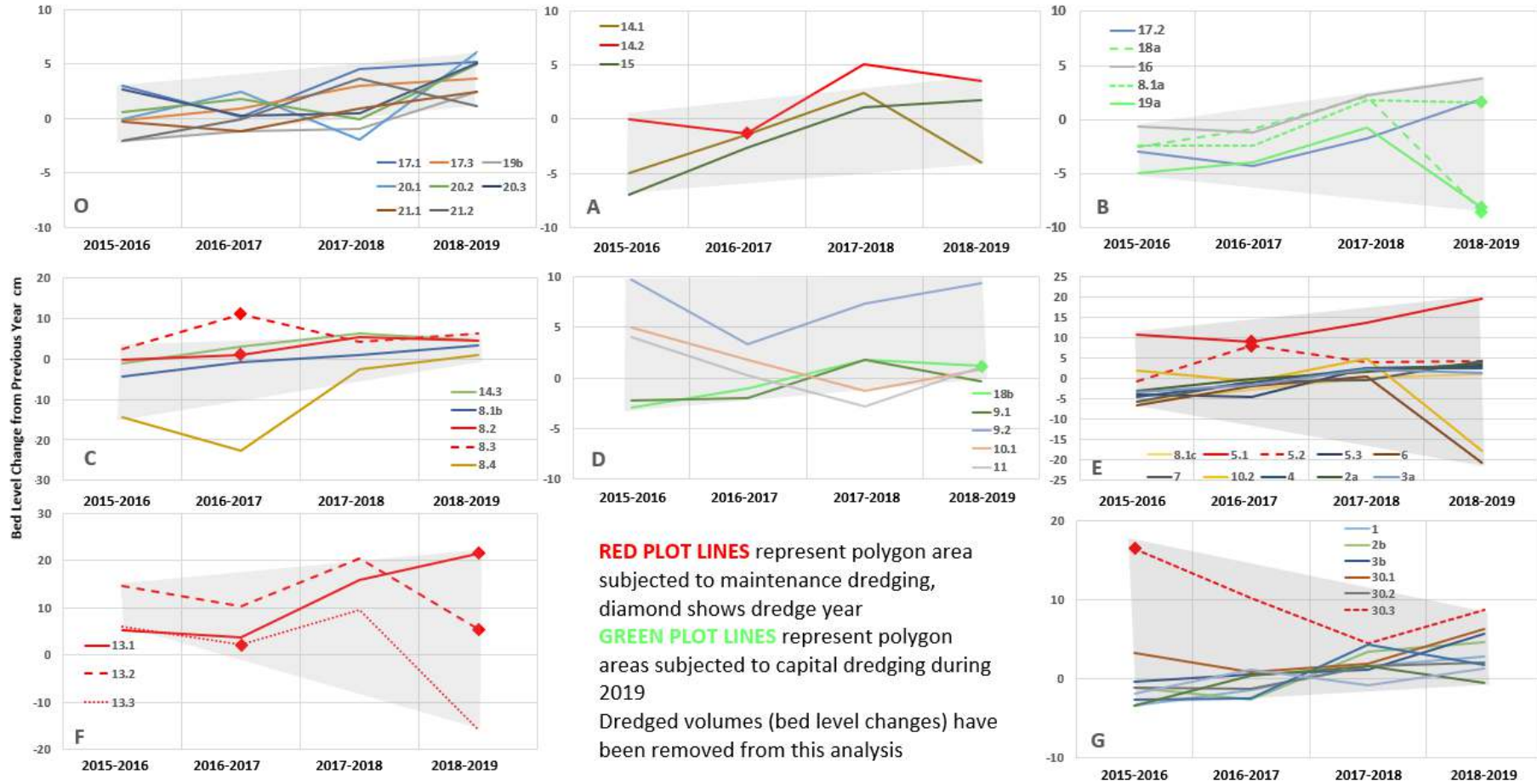


Figure 19. Change in bed level (cm) in all sub-polygons between annual surveys, grouped by sediment-flux polygons (O, A-G, Figure 1). See Table 5 and Figure 18 for identification of sub-polygon numbers. Note different y-axis scales. Dredging effects have been removed. Grey zone shows 'envelope' of conditions between maximum and minimum values per zone in 2016 and 2019.



The most notable changes compared to the 2018 rates of bed level change are as follows (> five-fold change in rate, Table 5, dredge sites excluded):

- | | |
|---|--------------|
| a) Solent Shore: Mid Shrape (20.2) and East Shrape (20.3), sand accreting | x 42-12 fold |
| b) Car Ferry Terminal (sites 6 & 10.2) accelerated erosion | x 36-7 fold |
| c) South of Chain Ferry East Bank accelerated deposition | x 5 fold |

These few sites with a marked (>5-fold) change in erosion/deposition have been explained above, with the exception of c) which showed a small volume change (<500t) and may be highlighted spuriously. The changes seen at b) (ferry terminal) may relate to the impact of creating/using the new berth for the commercial-vehicle ferry service during 2019.

In Figure 19 the average change in bed level within each sub-polygon, over each year since 2015, has been plotted, with data grouped by fine-sediment flux polygon (Figure 1). The effects of dredging have been removed (by adding-back known dredge volumes). With five years of data it is possible that slow trends of overall change in sedimentary behaviour may be beginning to emerge from the data. A best-fit envelope has been (subjectively) created for each set of plots. The situation for each flux-polygon is:

- O.** A slow change from a mix of erosional and depositional sub-polygons towards all showing depositional behaviour. Mostly sand zones¹⁷.
- A.** Only three sub-polygons, but a possible trend from stable/erosion dominated to mixed erosion/deposition conditions.
- B.** A change from all sub-polygons showing erosion to a mix of erosion/depositional behaviour.
- C.** A change from nearly all sub-polygons showing erosion to all showing depositional behaviour.
- D.** No consistent pattern of change within the group, similar conditions at beginning and end.
- E.** With the exception of the recent deepening associated with the car ferry terminal, most sites show consistent change from slightly eroding to slightly accumulating conditions. .
- F.** All polygons in this marina zone show depositional history with little consistent change.
- G.** With the exception of the marina area, a change from conditions mostly dominated by annual erosion towards a situation where most sub-polygons now show deposition.

Despite the net trends in accumulation/erosion (dry tonnes per year, Table 4) showing no consistent trend towards increased mud accumulation in the estuary since 2015 and reduced accumulation rates compared to the 1992-2015 period, many of the individual small polygon areas appear to exhibit a persistent change from erosion-dominated towards deposition-dominated (Figure 19). The effect of these small zones is overridden by the larger changes in other polygons, specifically those subject to dredging (sections 2.2 & 3.2.2). This slow shallowing in unmanaged zones might be expected given that a) the harbour is significantly over-deepened from its natural state² and b) the recent emplacement of the offshore breakwater may be reducing the amount of erosive wave energy in parts the outer harbour. The rates of change in the increasingly accumulative zones are

¹⁷ It has been discussed earlier in this section that a combination of strengthened tidal streams (as a result of the breakwater construction) and storm wave impact are together likely to be responsible for the build-up of sand along this shoreface.



low, of the order of <2cm difference per year. The persistence of these trends needs to be watched into the future.

3.3 Fine-Sediment Flux

3.3.1 Experimental Options and Assumptions

Water Exchange. The availability of water volume flow information in the outer harbour using (the original) modelling flow data (MF) and the new observation-based flow data (OF) has been explained in Section 2.1.4. The observation-based data can be further subdivided into a manual reconciliation version (OFv1) and an automated reconciliation version (OFv2). With the latter, six boundaries with good observation data remain ‘fixed’ and flow is automatically adjusted across the remaining six (‘free’) boundaries to enable reconciliation of volumes. Some flexibility in the selection of which are designated ‘free’ or ‘fixed’ boundaries offered further sub-options (OFv2.1, OFv2.2, OFv2.3). The results of all five options have been compared.

Turbidity. In order to derive a 30 minute average TSS value for each profile (ab, bc, bf etc, Figure 1) an assumption has to be made about how the TSS values vary spatially between the four turbidity measuring sites. The (simplest) model of linear variation through space was used with the 2016 data: If the centroid of a profile was within 50m of a turbidity measuring site, then just the data from that measuring site was used. Otherwise, the TSS concentrations at boundary centroids from the 2 or 3 closest measuring sites were combined, weighted according to the inverse distance to the sensors (closest sensor had the greatest influence). During the analysis of the 2017 data this simple approach was modified slightly, for four profiles where the presence of a recirculating gyre complicates the situation and periods of the tidal cycle were identified when an ‘upstream’ selection process best replaced the linear gradient approach. For 2019 the simpler approach was again reverted too, but this time the ‘average TSS’ value was determined for each end of each boundary, then averaged to give a value for the whole profile. Only the latter model has been assumed during the analysis of the 2019 data.

Sediment dry density. The fine sediment flux method calculates sediment flux in dry tonnes (derived from mg l^{-1} TSS measurements). The bathymetry surveys measure changes to the bed by volume however. In predominantly mud, or muddy gravel zones values of 0.6 or 0.8 t m^3 were applied to the volumes of bed sediment, the former to depositing beds and the latter to eroding beds (Section 2.1.5). Although based on field observations, these densities are an approximation, which must be recognised when reconciling flux-based and bathymetry-based data. In future a more precise approach could be developed, but for the 2019 data only the assumption based upon the above-identified values identified has been relied on.

Boundary mn. Based on the turbidity model and sediment dry density values described above, all five water-exchange options gave ‘reasonable’ fine sediment flux results, with exception of polygon E. The methodology consistently over-predicted the amount of fine sediment retained in this polygon. The method used in 2016/2017 showed the same shortcoming, but the cause of the error was not clear at that time as polygon B showed a large error too. In 2019 significant difference was confined to polygon E. Looking to correct the error by passing sediment into polygons A-D or F would only imbalance the good results seen there. Altering the balance of flux between polygons E and G is more feasible however, for the following reasons:

- We do not know the sediment volume retained in G from bathymetric data as surveys do not encompass the whole upper estuary (only to Folly Point). Diverting sediment from E to G therefore does not provide a conflict with known data.



- Water flow observations (new data⁶) across boundary mn (~chain ferry narrows) show a strong lateral asymmetry of flow. On the east side, where the turbidity sensor is situated, the water is shallower and flows more slowly, often with recirculating flow. On the west side the water is deep and shows stronger and more persistent flow.
- The strong flow differences across a short boundary seen at mn is not found elsewhere in the estuary. For this reason, the turbidity distribution assumptions (see earlier in this section) may not hold at this location. If this is true minor (<20%) variations in the turbidity levels applied to this boundary could be present, causing large changes in the estimates made of sediment flux passing in and out of the upper estuary, effectively correcting the imbalance seen in polygon E.

This hypothesis was tested, and it was found that by applying a 10-20% increase¹⁸ in the flood turbidity values observed at boundary mn, a correct sediment retention weight could be achieved in polygon E with a believable retention value still being seen in polygon G (upper estuary). This assumption has been adopted for the analyses reported here. At the same time it is recommended that in future the MMC Divers turbidity sensor site is moved to the CHC petrol barge, located on the western side of the polygon boundary, to confirm whether a slightly different turbidity regime is seen on the western side of the profile, and whether this difference resolves the issue.

3.3.2 Patterns and Processes of Fine-Sediment Flux

Polygon	Target	Option MF	Option OF-v1	Option OF-v2.1	Option OF-v2.2	Option OF-v2.3
A	-329	-4,034	-2,317	-1,876	942	942
B	-3,211	-11,029	-5,602	-7,077	-5,400	-8,007
C	827	-2,815	21	-28	582	582
D	1,275	464	886	1,354	1,354	1,354
E	-388	1,659	-780	-87	-87	-87
F	721	-155	-94	313	313	313
A-F	-1,106	-15,911	-7,886	-7,401	-2296	-4,903
G	-173	7,779	3686	3,686	3,686	3,686
Above Folly	3,859					

Table 6. Fine-sediment flux calculation results, in dry tonnes per year. Target values (left) are from bathymetry data (with +0.012m correction). All sediment flux values for polygon G apply a 1.2 correction factor to the turbidity data (see text), all other polygons have no adjustment.

The fine-sediment flux results for the five water-flow options are provided in Table 6. It can be seen that water flow option MF (from the original ABPmer model predictions) gives by far the worst representation of the target (bathymetry-derived) tonnages. Option OF-v1 (based on observed flows, manually corrected to align with known volume changes) gives the second-worst set of predictions, much improved over the MF option but with large discrepancy in polygon A. Option OF-v2 (based on observed flows with automated volume corrections permitted at six of the twelve boundaries) gave the best-fit results, with v2.2 superficially appearing to give the very-best set of predictions. However, full exploration of the data suggests that option OF-v1 gives a better fit when considering the flow variation imposed on the 'free' boundaries (i.e with this option automated flow volumes remain closest to the observed volumes). This option (see map in Figure 20, free boundaries

¹⁸ Or reducing the ebb turbidity by 10% and increasing the flood turbidity by 10%, equivalent to changing 10 mg l⁻¹ to ~9-11mg l⁻¹.



shown as dashed, fixed boundaries heavy solid lines) allowed boundaries ab, fg and de to be free in the lower harbour (with boundaries hi, hl and ik being free in all v2 options). This arrangement permits unconstrained flow of water through polygons A, C and E. Comparisons of the observed and 'automatedly modified' flow for this option are shown in Figure 20 (for an average tide), where it can be seen that patterns of flow remain generally similar to those observed, but volume exchange quantities are enhanced at times, consistent with the suspicion that (logistical) inability to deploy the current meter in the deep water navigation channels limited the chance of capturing full flow values.

From these results it is evident that errors in generating the water-flow exchange between the polygons can have large impact upon the fine-sediment-flux tonnages predicted, and replacement of the original model-sourced data with observation-based data has greatly improved the accuracy of the flux calculation process. However, comparing the 'target' tonnages of Table 6 with the proposed best-fit (Option OF-v2.1) flux model tonnage output it can be seen that the tabulated tonnages, although of the correct order of magnitude, are not exactly the same. It is important to recognise that the differences may derive from either side of the comparison, with localised multibeam variability and sediment dry density variability causing errors on the target (bathymetrically-derived) tonnages, and the detail of TSS concentrations and water volume exchange values leading to variability in the sediment flux calculations. At this stage in the development of the fine-sediment-flux monitoring project, it has been thought that on balance, errors involved in the bathymetric bed-volume changes were likely to be less significant than those derived from various assumptions made in the flux-modelling process, and that it should be the flux-calculation figures that should be modestly 'adjusted' to align the two sets of predictions. This adjustment was practically achieved by incorporating into the flux-calculating spreadsheets the ability to multiply the TSS values observed on the 'free' profiles by a small amount (shown for Option OF-v2.1 in the 'TSS adjust' columns on the right of Figure 20). With Options OF-v2 and OF-v3 an adjustment of ~20% was required for polygon A and polygon B respectively, as a result of having a 'fixed' flow through boundary fg. With option OF-v1 however (Figure 20) the all adjustments needed¹⁹ lay in the range $\pm 7\%$, suggesting a much more accurate representation of the true water exchange is achieved by assigning profile fg as 'free' (probably due to the absence of current meter data at the deeper, fairway end of this important boundary).

In Figure 21 the fine-sediment flux tonnages are converted to bed level changes, for both the raw flux data (thin lines) and the flux data reconciled to the known bathymetric volume changes (thick lines), with the envelope encompassed being shaded (negligible difference for polygons D, E and G). In Figure 22 the reconciled tonnage changes through 2019 are plotted. Comparing the two figures emphasises the effect of the size of the polygon relative to the tonnage change, in determining the effect on bed level. Polygon G for example (very large area) showed less than 1cm bed level change though the tonnage accumulating was ~3,500 t.

The successful reconciliation of the bathymetry-change data and the fine-sediment flux data provides three positive steps forward in the Medina sediment management project:

1. Giving confidence that the correct sets of assumptions have been made in dealing with the complex (bathymetry/flux) data sets, and that the resulting reports of how the estuary floor is changing each year are realistic.

¹⁹ Excluding boundary mn, which was permanently set at 1.2 (20%) adjustment factor at an early stage in the sediment-flux-measuring process.



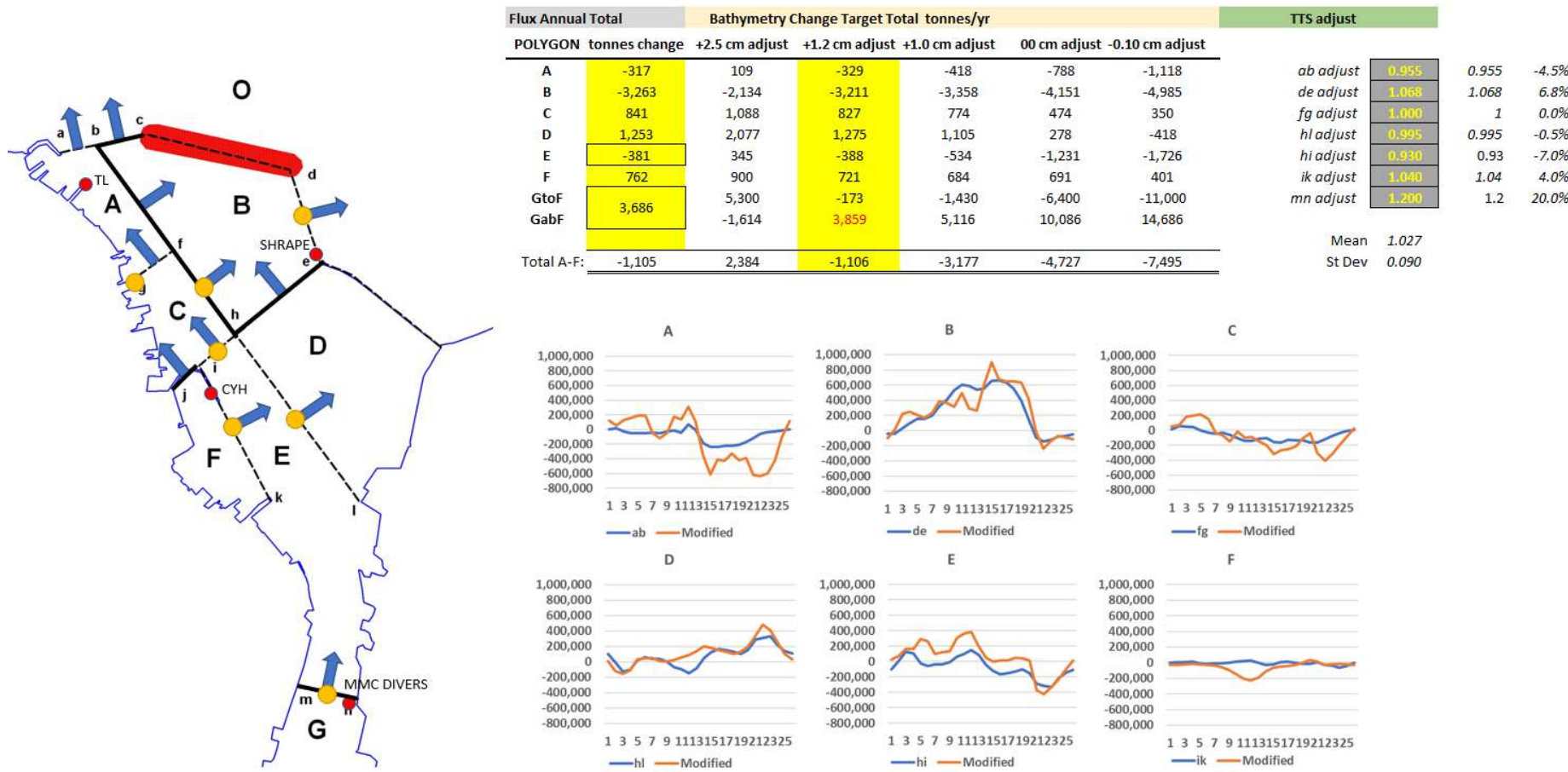


Figure 20. Option OF-v2.1 details of fine adjustment to integrate sediment flux metrics with bathymetric change metrics. Table at top shows adjusted flux tonnages per polygon (shaded yellow on left) and bathymetric tonnages for all bathymetry QC adjustments to the right (yellow shaded is used +0.012m correction). TSS adjust on far right shows final adjustments to TSS concentrations used to generate a near-perfect fit between the flux and bathymetry metrics. Graphs below compare observed (blue) and used ('modified') water flow through the six 'free' boundaries for this option on a mean tide (2.75m range).



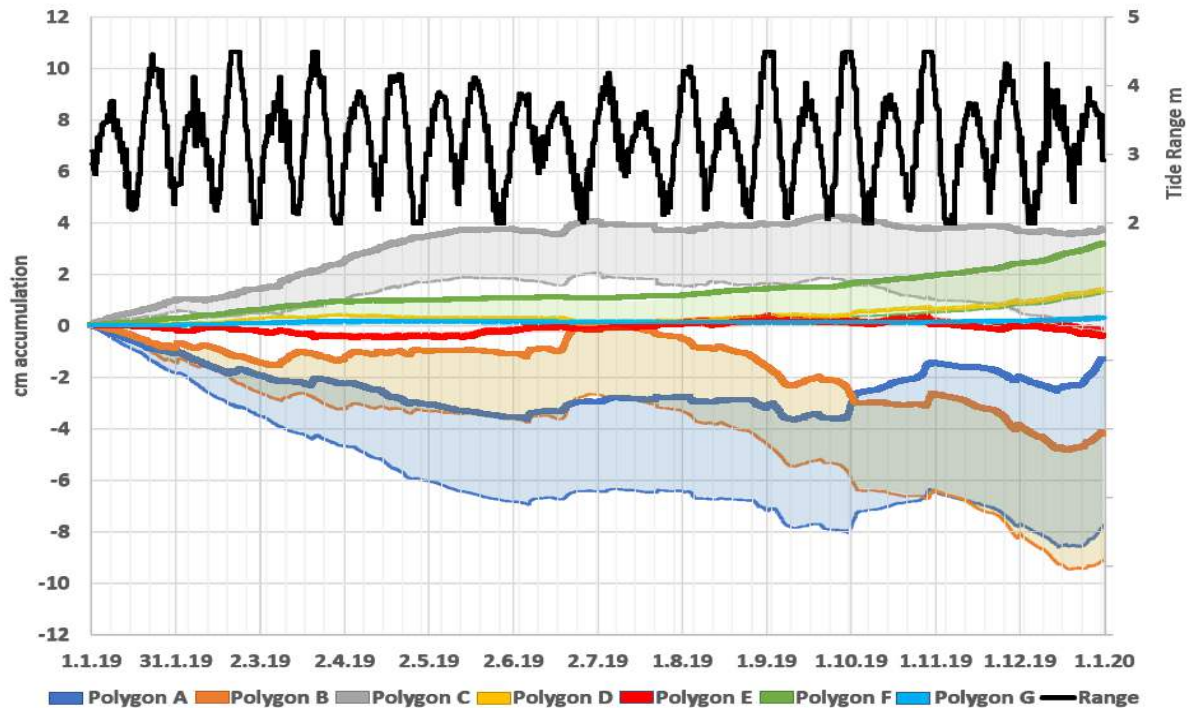


Figure 21. Cumulative mud accumulation (in centimetres) through 2019 in each polygon. Thick lines are the bathymetry-volume adjusted data, the thin lines the unadjusted fine-sediment-flux model output (shaded areas connect the two lines). For polygons D, E and G the two datasets are near identical. Black plot (top) shows the variation in tidal range through the year.

2. Confirming the hoped-for possibility that in future the data processing for the fine-sediment-flux monitoring can be automated (with software development) to give useful on-going reports through the year (weekly/monthly) of the state of fine sediment erosion or accretion in each of the seven polygon zones. Manual cleaning and fine-adjustment of the data output (reconciliation with the bathymetry-change data) can be undertaken at the close of each year to provide the most precise results possible for each annual report.
3. As can be seen from Figure 21 and 22, the fine-sediment flux data reveal how patterns of accumulation/erosion of mud vary between polygons for different times of the year. This variability must relate to the different processes that are active, as discussed below. Appreciation of key timings for change will enhance the ability to optimise management activities in terms of minimising dredging costs and impacts.

The time-series of accumulation/erosion history seen in each polygon of Figure 22 can be summarised and potentially explained as follows:

Polygon G: Upper estuary south of boundary mn. Net accumulation at end-of-year. Comparing the plot in Figure 22 with the annual TSS variation seen in Figure 4-6 it would seem that the upper estuary responds primarily to the winter supply of fine sediment from the wider Solent and adjacent English Channel areas, although mud eroded from the bed of the outer estuary in winter (polygon B specifically, Table 4) will have contributed. Strong accumulation is seen January-March, tailing off through April, then recommencing mid-October to rise again through November-December. Through the summer/autumn period slight erosion replaces accumulation, as tidal, summer-boating and summer-storm activities encourage mud resuspension and dispersion on the ebb, overcoming



the much reduced summer mud supply from offshore. From the bathymetric change (Table 5) we know that the latter processes have favoured erosion across the intertidal sub-polygon areas north of the Folly Inn (deposition in the marina zones and other sheltered subtidal areas being offset by intertidal erosion, with little net change for the zone as a whole), with most annual accumulation occurring in the uppermost and shallowest estuary reaches south of the Folly Inn.

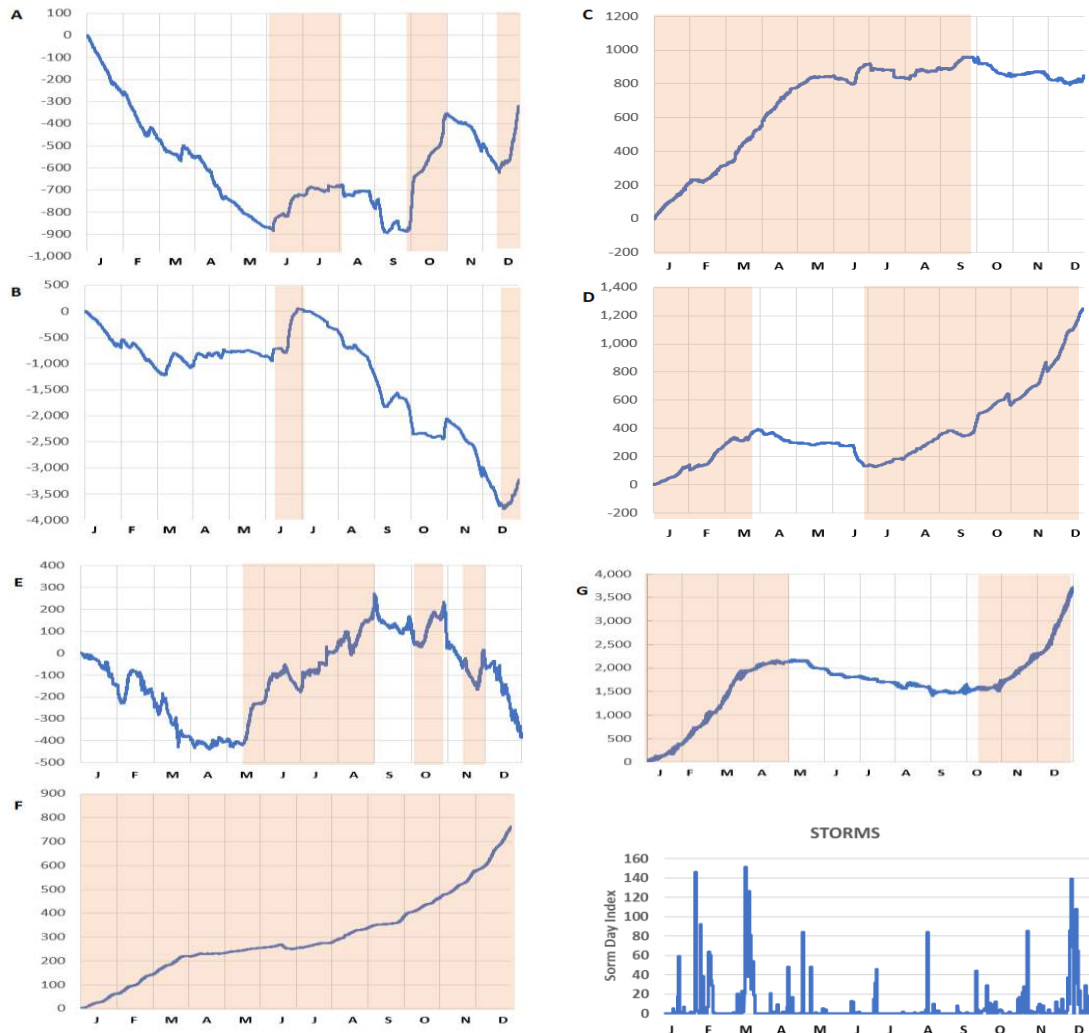


Figure 22. Fine-sediment flux model output, reconciled to the bathymetry-volume change data, showing cumulative dry tonnes accumulating through 2019 per polygon. Main periods of accumulation are shaded in pink. The distribution of storm days/intensities through 2019 is shown bottom right.

Polygon F: Cowes Yacht Haven and adjoins. Net accumulation at end-of-year. An over-deepened area, known to be a zone of persistent accumulation. This zone shows the same response as polygon G, with strongest accumulation January-April and October-December. Hardly any erosion occurs during the summer period, attesting to the absence of erosion processes in this very sheltered zone, and slow accumulation continues, fed from the reduced offshore supply and the reworking of mud from other estuary zones (notably polygon B). The overall amount of sediment accumulated during the year is lower than would be expected from both the dredging history, and 2019 being a year of slightly enhanced mud supply from offshore. This observation is most likely attributable to the effects of the dredging of this area that occurred early in the year, which both



potentially affected the bathymetry-change volumes (difficulty in assessing exact dredge volumes extracted) and permitted a slow readjustment/reworking of the dredged bed through the year, which will have affected the flux results.

Polygon D. Intertidal flats and subtidal mud zone east of the main fairway and sheltered by Shrape Breakwater. Net accumulation at end-of-year. Known zone of persistent accumulation affecting most parts. Another winter-dominated accumulation zone, similar to polygons G & F, but showing accumulation January-March then July-December. Between April and June erosion occurred, as a result of the diminished mud supply at that time (from both offshore and the winter erosion that occurred in polygon B), and probably the erosion effects of summer storms and shipping activity, and also most probably showing erosive recovery effects from the dredging of the NW corner of this polygon during the Eastern Approach Channel dredge project early in the year.

Polygon C: West Cowes estuary shore. Net accumulation at end-of-year. A zone that has changed from slight erosion to slight deposition over the previous four years (Table 4, Figure 19). From January to April 2019 this zone saw steady accretion, which then stabilised to a situation of little change until the close of the year. The annual influx of fine sediment from offshore and from erosion in polygon B could have driven the early accumulation, augmented by some spillage of mud from the large dredging project in the Eastern Approach Channel, directly upstream from C on the flood tide. The slight erosion that persisted through October-December must be due to the presence of erosive energy (storm waves, shipping) overcoming the influx of offshore/local mud. Considering the history of slight annual erosion at this site, the late year situation may in fact be more normal for the zone, and the early-year accumulation may reflect mostly mud dispersed into the zone from the recovering dredge site in polygon B.

Polygon E: Main fairway, south outer harbour. Slight net erosion at end-of-year. Historically a mixed zone, mostly stable, with erosion (scour) associated with the car ferry terminal, and persistent deposition within the (sheltered, over-deepened) Shepard's Wharf marina. The pattern of change in the polygon shows an inverse response to sedimentation processes observed in polygons C, D, F & G above, showing erosion from January to April and then again from September to December, with accumulation through the summer. It is difficult to image storm conditions affecting sedimentation in this part of the harbour, being deep, sheltered from the influx of Solent storm wave and having no local wave fetch (narrower and has wharved margins). Similarly shipping activity is unlikely to produce reduced energy input through the summer. The April-September period covers the time of the lowest spring tides of the year (<4m, Figure 21) therefore the absence of a very strong peak-spring flow period each month at this time may encourage temporary accumulation. A further observation is that the polygon holds a reciprocal relationship with polygon G, the upper estuary. When G is accumulating E is eroding, and *vice versa*. Polygon E may act as an effective throughflow corridor for mud into polygon G during the winter months, with mud kept moving by the periodic scour of very high spring tides, then be a recipient for mud lost from polygon G during the summer period when highest tidal flows are absent.

Polygon B. Central outer harbour containing the new Eastern Approach Channel. Net erosion at end-of-year. Historically an eroding zone, with higher than normal erosion rate in 2019. The polygon generally shows steady erosion through the year, with a more stable period from April-July. The zone erodes slowly through the winter-spring-autumn periods, under the influence of tidal scour and storm waves (from NW to NE). The irregularity of change seen during 2019 (Figure 22) may be due to the effects of the January deepening of the eastern Approach Channel, with slow continuing dispersion of material spilt locally during the dredge, and slow adjustment of the channel side-



slopes, resulting in a complex picture of entrapment and release seen in the irregular pattern of fine-sediment flux through the polygon. This zone is also still adjusting to the emplacement of the offshore breakwater in 2015-16, with diverted tidal streams causing local minor alterations in bed morphology.

Polygon A. Western shore of the outer harbour and main fairway. Slight net erosion at end-of-year. Erosion has been persistent here through the four years of the project but at a steadily decreasing rate. The area is open to storms from the NW to NE, being just inside the harbour entrance, and erosion persisted steadily through the storm events that were present January-May 2019, totally overcoming the winter influx of mud from the wider Solent region at this time. As with Polygon E, some deposition occurred June-July, perhaps attributable to the lessened power of the top spring tides at this time. The zone then showed alternating periods of deposition and erosion through the autumn and early winter, perhaps explained by the zone accumulating mud coming from offshore and also erosion in polygons B & E, which was periodically moved out again under the effect of local winter storms.

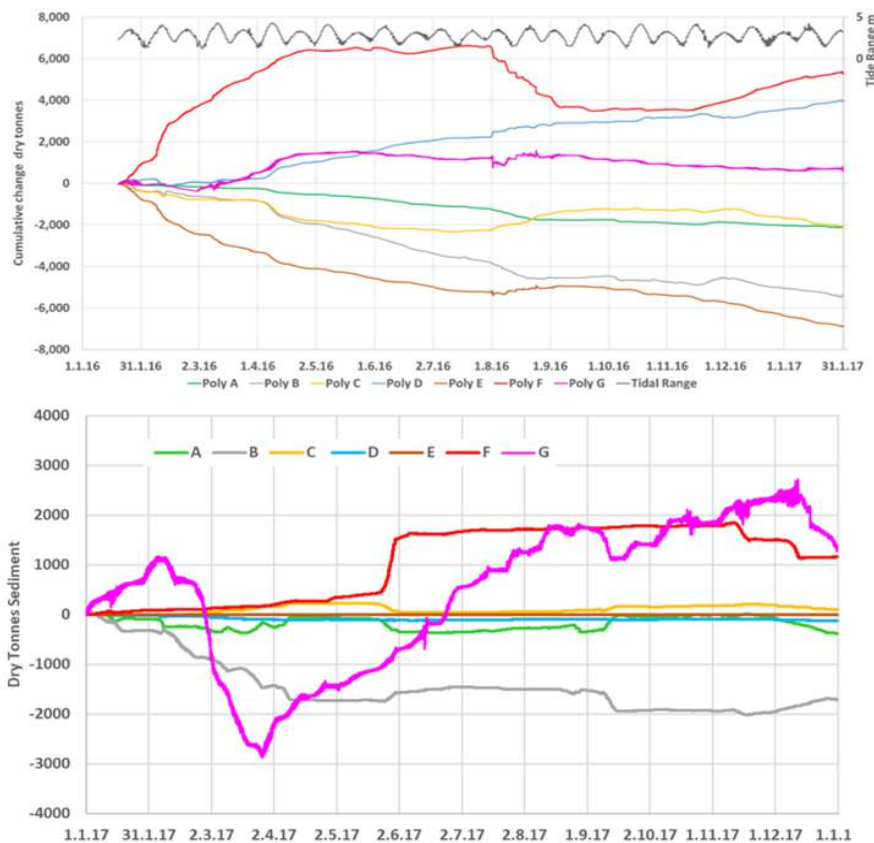


Figure 23. Fine-sediment flux results from 2016 (top) and 2017 (bottom).

Measurement of the flux during the year of fine-sediment through the seven polygons was first undertaken in 2016 and then again in 2017, but no attempt was made in 2018 due to the poor quality of the turbidity records. In 2016 and 2017 there was very poor agreement between the sediment-flux data and the bathymetric-volume-change data for the polygons, due primarily as we now have established to the inaccurate water-exchange data used, but also attributable to the poorer quality TSS data (frequent occurrence of biofouling, loss of data for other reasons) and also to the poor representation of sediment exchange through the chain-ferry narrows, as is now suspected and being corrected for. Irrespective of the poor correlation between the flux and



bathymetry-change results in 2016 and 2017, the flux data were simply aligned with the annual bed-volume changes from the bathymetry surveys, in order to explore the temporal aspects of the changes found in each polygon. The results for the two years are shown in Figure 23. Despite the unconfirmed assumptions used in producing these results, and despite the poor quality TSS data (particularly noted in 2017, with sharp and difficult to explain changes in the flux plots) the general patterns revealed then are consistent with the more reliable 2019 data (Figure 22).

- Polygon A. Winter erosion reduces in summer with some accretion periods, net loss of mud over the year.
- Polygon B. Winter erosion reduces in summer with some accretion periods, net loss of mud over the year.
- Polygon C. Variable erosion/accumulation conditions alternate.
- Polygon D. Accumulation dominates, stability/erosion at times.
- Polygon E. Steady erosion, stronger in the winter months (little apparent change in tonnages through 2017?)
- Polygon F. Net accumulation over the year with strongest accumulation in winter (lot of spurious data seen in 2017?).

It has been possible to interpret the flux patterns seen in 2019 much more confidently than those generated in previous years, due to the consistency now seen between the bathymetry-change and sediment-flux results (derived principally from improved simulation of water flow). With continued bettering of our understanding of field variables (primarily now focussed on moving the MCC TSS sensor to the Petrol Barge) and continued effort to improve maintenance effectiveness (swift response to biofouling, establishing more reliable power supplies) the 'tweaking' factors used in the reconciliation process will become smaller and the cause/effect relationships involving the many processes that drive fine-sediment flux can become increasingly understood.

4. Conclusions and Recommendations

Methodology. The project to measure the dispersion of fine-sediment into, out of and around the Medina estuary was initiated at the beginning of 2016. This report covers the fourth year of monitoring, from 1/1/2019 to 31/12/2019. Throughout the first three years of the project, maintaining the quality of the Total Suspended Solids (TSS) data was problematic due to strong summer biofouling, staff availability for no-delay maintenance and intermittent power supplies. These issues were addressed at the end of 2018 by the installation of GPRS loggers at the four TSS sensor sites, thus providing near real-time access to the data from the office. This step, accompanied by improved anti-biofouling measures, has significantly improved the data-capture rate during 2019.

In addition to these turbidity monitoring issues, the ability to deliver on the experimental fine-sediment flux part of the project was seen to be problematic from the end of the first year, with difficulty found in reconciling annual changes in bed levels in the estuary with data on exchange of fine-sediment flux between sub-sections of the estuary. One potential cause of the difficulty was the information on water-volume exchange within the estuary, vital to the flux-calculation process, and initially derived from a mathematical model of the estuary. During 2019 a current meter was deployed at sixteen sites around the estuary, over spring-neap cycles, and an observation-based dataset of water flow around the estuary created. This new source of water-volume exchange measurements has proved to be much more realistic than the output from the model originally relied upon, and allows much more confidence in the experimental approach being developed. The current meter measurement programme has also allowed identification of a potential fault in the



original programme design. An initial assumption made was that water flow velocities within the harbour did not show sharp variation at any locality, and therefore that location of the TSS monitoring sites was not critical to specific localities, and could rely on a model simulating smoothly varying TSS values between the sensor sites. The current meter data showed that this situation does not apply in the narrow main channel immediately south of the chain ferry. Water flow observations on either side of boundary mn showed very different conditions with much stronger, persistent flow against the western bank. To date the TSS sensor for this area has been located against the eastern bank, and the data it generates is therefore thought to be possibly unrepresentative of the whole-channel conditions. As a result, it has been recommended that the MMC divers TSS sensor be relocated to the CHC petrol barge on the opposite side of the channel. This change will take place during June 2020, and should improve the ability to simulate the flux of fine sediment between the upper estuary (above the chain-ferry narrows) and the outer estuary. Other recommendations, made in previous years, concerning the installation of a fifth turbidity sensor in the vicinity of Kingston Wharf (upper estuary) and a turbidity sensor in open Solent waters (to monitor the seasonal regional mud source) remain viable but have not been addressed.

Sources of Mud. Sedimentation within the Medina estuary is dominated by the accumulation of mud with minor amounts of fine sand. Analysis of the 2019 TSS data confirms that, as previously thought, the annual pattern of turbidity is dominated by the seasonal (autumn/winter/spring) influx of fine, clay-rich sediment generated by storm-wave-driven erosion of clay strata from the shallow waters of the English Channel from Poole to Selsey²⁰. The Channel winter storminess was slightly above average during 2019, with most activity seen in November and December. The influence of this offshore supply, strongest later in the year, is seen on the annual plots for the four sensors (data averaged for each of the 25 spring neap cycles through the year) in Figures 5 & 6, and in the annual variation in the rates of accumulation of mud in the 'depositional' polygons (e.g. polygon F, Figure 22).

Despite the importance of this offshore mud supply, local sources of mud, derived principally from bed erosion of Holocene silt-rich deposits flooring the estuary (notably in polygon B) are generated as a result of tidal scour on peak spring tides, combined with winter storm-wave activity in the outermost harbour. Previous monitoring reports noted an increase in this rate of erosion in polygon B in 2016 compared with earlier years (Table 5), and attributed the change to adjustment resulting from the emplacement of the new offshore breakwater in that year. The breakwater will have modified wave and tidal energy slightly in different zones, causing some readjustment of bed levels and consequent increased mud flux. Through the recovery years of 2017 and 2018 this erosion in polygon B decreased, to the point of modest accumulation occurring in 2018. In 2019 the erosion in polygon B (and hence the increased release of reworked silt-rich Holocene mud) has again substantially increased, possibly a continuing response the breakwater's presence but more likely as a result of the extensive dredging project that took place in February, opening up the new Eastern Approach Channel. This project cut extensive raw new surfaces into the Holocene mud deposits that underly the estuary bed, which during the months of recovery post dredging will have been a source of fine suspended sediment, particularly during peak tidal flows and winter storms. Thus the offshore supply of mud to the estuary will have been slightly augmented by this local supply during 2019.

The contribution of these two sources to the mud deposits of the estuary can be determined from particle-size analysis, with clay-rich (offshore) and silt-rich (local) deposits being differentiable.

²⁰ Demonstrated from satellite imagery in previous Ambios reports.



Analysis of grab samples collected in early 2017 showed an increased representation of (local) silt-rich muds over the offshore (clay-rich) source, as a result of the erosion initiated by the breakwater emplacement. No grab samples were collected in 2018 or 2019, but it is recommended that a few key locations are sampled towards the close of 2020 and particle-size analyses of the mud fraction undertaken, in order to confirm this situation.

The Total Suspended Solids Regime. The all-sites mean TSS value was 11.5 mg l^{-1} in 2019, significantly lower than in previous years (15.1 in 2018, 14.0 in 2017 and 15.2 in 2016). The 2016-2019 annual distribution of all-sites averaged TSS values (averaged by successive spring-neap cycles) shows this marked reduction in TSS values in Figure 3, and shows that standard deviations as well as means have decreased. For this reason it seems most likely that the lower TSS values recorded represent an improvement in quality if the data (reduction of the effects of biofouling) rather than a significant change in the regime.

Individual TSS readings can be as low at $<1 \text{ mg l}^{-1}$ (mid-summer, neap conditions) and reach about 200 mg l^{-1} (local storm conditions, spring tide, winter). Data averaged by spring-neap cycle (~ 14 days) typically show variability over the range $5\text{-}40 \text{ mg l}^{-1}$ between high/low energy/supply conditions.

Results of the analysis of the data collected during 2019 remain consistent with the model of processes of sediment circulation identified in the 2015/2016 surveys and from the initial years of monitoring. The key features of this suite of processes are:

- A seasonal variation in the supply of mud to the estuary, mostly fed from offshore sources but also derived from local erosion within the estuary under peak tide/wave/dredging action.
- Tidal energy is the primary process distributing this mud influx around the estuary. Most tidal reworking of mud occurs over spring tides, with little bed resuspension occurring through neaps. Most spring-tide-driven reworking, causing an elevation of TSS levels, occurs through the winter periods of strong mud supply, and results in the reworking of mud into the most sheltered parts of the estuary. During the summer period, this mud supply becomes exhausted, and spring tide energies are less effective in elevating TSS levels.
- Local storm conditions also elevate TSS concentrations, by a factor of about 100% above normal tidal processes in exposed areas (e.g. Shrape) down to about 25% in sheltered zones (e.g. CYH). These storms may both cause new erosion of the bed in certain areas (particularly polygon B) and also drive the sweeping of offshore-derived mud, temporarily accumulated, into more sheltered areas.
- Shipping effects (ships, car ferry, Red Jet, leisure boating) can be identified as agents of scour, enhancing TSS levels with their activity. At certain times, the effect of shipping (particularly high-density operations such as ferries) can cause an elevation in TSS comparable to local storm impacts.
- Dredging during early 2019 did not cause extensive, identifiable plumes of increased TSS, but probably caused protracted, low-level increases in reworking by tidal scour as 'raw' dredged surfaces settled and stabilised during months of 'recovery'.

Fine-sediment retention. During 2019 the estuary accumulated some 2,500 dry tonnes of mud (Table 4), with some 1,100t being eroded from the lower estuary (north of the chain ferry narrows) and 3,700t accumulating upstream of the Chain Ferry narrows, mostly in the subtidal/marina areas and in the very uppermost reaches (above Folly Inn). Dredging records (post 1987) indicate that the 'status quo' has been historically maintained in the Medina Estuary with an averaged removal of



about 10,000 dry tonnes of mud each year (Appendix 2). 2019 was therefore a year of below normal accretion.

This compares with 2016 (the only year we have whole-estuary data) which saw a loss of about 10,000t (Table 4). 2017 and 2018 may have shown nearer to normal amounts of mud retention. Given that 2019 was a year of slightly above average offshore storminess (processes generating the offshore winter mud supply) the low level of accumulation is considered unusual. The change could be due to the dredging that took place in 2019, simply as a result of the difficulty in quantifying precise dredge removals, and also due to recovery of the extensive mud dredge zones (primarily in polygons B and F) through processes of stabilisation of the dredged surfaces, notably the dispersion of material disturbed or spilt but not removed at the time of dredging.

The accumulation seen through 2019 in various localities (polygons D, F and subtidal G) will have been partly fed from erosion zones within in the estuary, supplementing the main influx from offshore, and also from (low) river input. As has always occurred, the main zones for mud accumulation in 2019 were the marinas, with Shepard's Wharf and East Cowes marina seeing the largest accumulation. Polygon D (Shrape Flats inside the breakwater, sub-polygons 9.2, 10.1 and 11) was again a significant area of accretion, as seen in most previous years. The trend in many sub-polygons that were not dredged during the period 2015-2019 has been towards slightly increased accumulation over time (Figure 19), not increased erosion.

The substantive increase in sand accretion seen across the eastern approaches to the harbour (sub polygons 20.1 & 20.2) in 2019 is part of a process that seems to have started in 2015 (although not noted in 2018), with the zone showing slight erosion in previous decades (Table 4). This is a zone of sand transport under the combined action of tidal and wave currents, and the ABPmer breakwater EIA modelling predicted increased tidal flow through this shallow, partly intertidal zone as a result of the breakwater emplacement. Because of the large area of the zone bed level changes are modest (~+5cm) but this trend should be continued to be monitored in the future.

Dredging practices. In 2019 meetings and discussions were held between CHC, key stakeholders and scientific advisors, to consider the possibility of trialling water injection methods as a more sustainable approach to fine-sediment management within the estuary. This followed the update of the Medina Baseline document, and the issue of a discussion document on potential sustainable sediment practices in the estuary²¹ during 2018. Although a costed series of proposals were produced, and the full breadth of the issue discussed in some detail, no consensus has yet emerged to support the commissioning of a trial. Data produced by the fine-sediment monitoring programme continues to build a robust baseline of the TSS regime which can be evaluated by the regulators once local appreciation of the situation allows a move towards sustainable practices to take place.

²¹ https://www.cowesharbourcommission.co.uk/content/S636608808817933107/SUSTAINABLE_SEDIMENTATION_MANAGEMENT_IN_THE_MEDINA_ESTUARY_March_2018.pdf



APPENDIX 1. Listing of Excel Files Containing Analysis of Data for 2019 Fine-Sediment Flux Monitoring.

Name	Date modified	Type	Size
Backups_2019	10/04/2020 11:29	File folder	
Figures	15/05/2020 19:01	File folder	
01_TIDESTAGE_Analysis_2019.xlsx	21/05/2020 13:32	Microsoft Excel W...	57,058 KB
02_Hayling Island Historical.xlsx	13/05/2020 16:16	Microsoft Excel W...	21,537 KB
02_Milford-on-Sea Historical.xlsx	13/05/2020 12:07	Microsoft Excel W...	19,338 KB
02_Sandown Bay Historical.xlsx	13/05/2020 12:19	Microsoft Excel W...	20,871 KB
03_IOW_SWELL_WAVES_WEATHER_201...	27/03/2020 09:37	Microsoft Excel W...	20,546 KB
04_TURBIDITY_ORDER_CYH_2019.xlsx	27/03/2020 09:25	Microsoft Excel W...	18,267 KB
04_TURBIDITY_ORDER_MMC_2019.xlsx	06/04/2020 14:28	Microsoft Excel W...	19,231 KB
04_TURBIDITY_ORDER_SHRAPE_2019.x...	27/03/2020 09:23	Microsoft Excel W...	13,230 KB
04_TURBIDITY_ORDER_TL_2019.xlsx	02/04/2020 20:22	Microsoft Excel W...	18,085 KB
05_TURBIDITY_CALIBRATION_CYH_201...	31/03/2020 11:26	Microsoft Excel W...	39,152 KB
05_TURBIDITY_CALIBRATION_MMC_20...	06/04/2020 16:45	Microsoft Excel W...	37,794 KB
05_TURBIDITY_CALIBRATION_PORTAB...	08/04/2020 19:35	Microsoft Excel W...	4,872 KB
05_TURBIDITY_CALIBRATION_SHRAPE...	08/04/2020 19:38	Microsoft Excel W...	31,952 KB
05_TURBIDITY_CALIBRATION_TL_2019....	08/04/2020 20:09	Microsoft Excel W...	36,890 KB
06_TURBIDITY_STATISTICS_CYH_2019.x...	27/05/2020 15:06	Microsoft Excel W...	47,161 KB
06_TURBIDITY_STATISTICS_MMC_2019....	06/04/2020 18:15	Microsoft Excel W...	47,293 KB
06_TURBIDITY_STATISTICS_SHRAPE_20...	08/04/2020 20:04	Microsoft Excel W...	48,047 KB
06_TURBIDITY_STATISTICS_TL_2019.xlsx	08/04/2020 20:14	Microsoft Excel W...	46,951 KB
07_TURBIDITY_PLOTS_CYH_2019.xlsx	01/06/2020 13:20	Microsoft Excel W...	2,399 KB
07_TURBIDITY_PLOTS_MMC_2019.xlsx	01/06/2020 13:31	Microsoft Excel W...	2,317 KB
07_TURBIDITY_PLOTS_SHRAPE_2019.xlsx	01/06/2020 16:48	Microsoft Excel W...	2,070 KB
07_TURBIDITY_PLOTS_TL_2019.xlsx	01/06/2020 13:25	Microsoft Excel W...	2,166 KB
08_TURBIDITY_FILL_CYH_2019.xlsx	04/06/2020 17:28	Microsoft Excel W...	13,283 KB
08_TURBIDITY_FILL_MMC_2019.xlsx	04/06/2020 23:09	Microsoft Excel W...	13,571 KB
08_TURBIDITY_FILL_SHRAPE_2019.xlsx	04/06/2020 23:10	Microsoft Excel W...	13,101 KB
08_TURBIDITY_FILL_TL_2019.xlsx	04/06/2020 17:35	Microsoft Excel W...	13,193 KB
09_ALL_DATAtoFLUX_CENT_2019.xlsx	10/04/2020 11:09	Microsoft Excel W...	14,764 KB
09_ALL_DATAtoFLUX_PREV_2019.xlsx	10/04/2020 10:59	Microsoft Excel W...	14,700 KB



APPENDIX 2. Notes on allowing for dredging in sediment budgets.

This project has the task of monitoring the net accumulation/loss of mud from the Medina estuary bed. This note is concerned with the interpretation of annual bed level changes using GIS analysis, from precision multibeam data. The volume change per year per specific bed zone (polygon) is determined from that analysis. However, at times during each year in specific polygons dredging has artificially removed some of the bed (both capital and maintenance dredging). Since December 2015 this dredge volume has been allowed for in the analysis by adding back in the recorded dredge volumes per polygon. In this way the net natural build up or removal of mud is reported.

In Table 5 of the report the results of the GIS analysis are reported without this adjustment of adding back in the dredge volumes. In Table 6 the adjustment of allowing for dredging has been undertaken. In Table 6 the units of measurement have also been changed from cubic metres (measured by the multibeam surveys) to dry tonnes of mud. The conversion factors used are described in section 2.1.5. Thus Table 5 shows, for the post 2015 data, our best estimate of the weight of dry mud that has moved in or out of the various estuary areas solely under the influence of natural processes. The variability in man's efforts in dredging certain zones from time to time will result in those zones deepening or shallowing, but will not impact upon our estimates of natural mud flux.

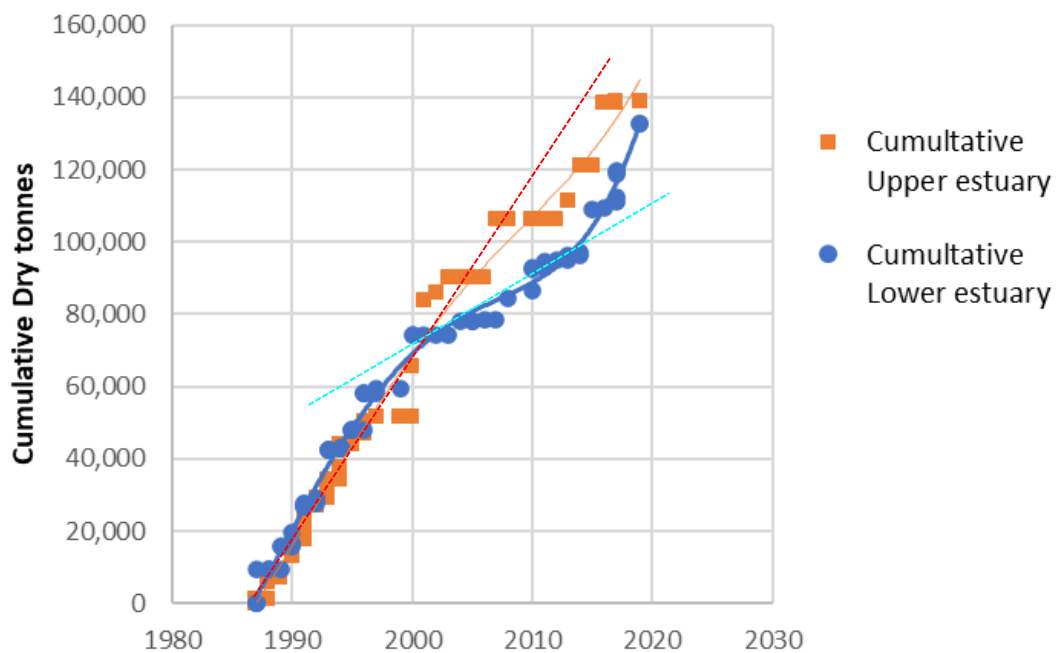
For data on bed level changes before 2015 a different model of interpretation prevails. The last extensive survey of the estuary bed pre-2015 was in 1992, and a single beam sounder survey. The GIS analysis conducted looked at the changes in bed level between 1992 and 2015, and added back in the dredge volumes from the various capital dredging that occurred through the period, occurring once only at a small number of specific sites. Clearly during that period a lot of maintenance dredging went on, repeatedly at the same sites, which could not easily be allowed for on the same basis. The 1992-2015 GIS analysis volume change, added to the capital dredging volumes removed, indicated that the net annual average change in the estuary bed volume over the 23 year period lay inside $\pm 500\text{m}^3$, the range reflecting both the imprecision of the earlier echo sounder survey and the inaccuracy of estimating dredge volumes from old records. This result indicates that over the period 1992-2015 the estuary bed levels did not vary much beyond the changes invoked by capital dredging, therefore the volume of maintenance dredgings exported through the period equalled the amount of mud naturally imported by the estuary system.

The figure below shows the history of maintenance dredgings disposal at sea from the Medina estuary over the period 1987 to 2019, separated into upper and lower estuary sources (above and below the chain ferry). Based on the logic in the previous paragraph, for the period prior to 2015 (since when a new more precise method is being followed) these tonnages also represent the import of mud into the Medina estuary, mostly from offshore. Guided by the red and blue rate lines fitted to the data, it can be seen that prior to 2000 both the upper and lower estuary imported mud at similar rates, ~5000 dry tonnes per year each totalling ~10,000 dry tonnes per year for the estuary as a whole. From 2000 the lower estuary rate of maintenance dredging export/natural mud import appeared to slow to about 2000 dry tonnes per year, with the upper estuary continuing at near 5000 dry tonnes per year. Since 2010-2015 the maintenance dredging yield from the upper estuary has tended to slow, whereas that from the lower estuary has regained its previous rate.

Using regression lines fitted to the rate of maintenance dredgings disposal as a proxy for the naturally driven influx of mud to the estuary, as has been done here for the pre-2015 period, is at



best only an approximation of reality, and breaks down totally if plough and WID methods are used (as was trialled in the period 2010-2015 in the Medina at some sites). The precision methods used today (paragraphs one and two above) provide a much more reliable metric for fine sediment flux, covering in detail processes of change across the whole estuary and highlighting the considerable variability in process rates that occur from year to year.



Maintenance dredging history in the Medina estuary since late 1980's.

Red dotted line approximates 5,000 dry tonnes per year, blue dotted line approximates 2000 dry tonnes per year.

